



**University of
Zurich** UZH

**Zurich Open Repository and
Archive**

University of Zurich
University Library
Strickhofstrasse 39
CH-8057 Zurich
www.zora.uzh.ch

Year: 2005

Unequivocal delineation of clinicogenetic subgroups and development of a new model for improved outcome prediction in neuroblastoma

Vandesompele, J ; Baudis, Michael ; De Preter, K ; Van Roy, N ; Ambros, P ; Bown, N ; Brinkschmidt, C ; Christiansen, H ; Combaret, V ; Lastowska, M ; Nicholson, J ; O'Meara, A ; Plantaz, D ; Stallings, R ; Brichard, B ; Van den Broecke, C ; De Bie, S ; De Paepe, A ; Laureys, G ; Speleman, F

DOI: <https://doi.org/10.1200/JCO.2005.06.104>

Posted at the Zurich Open Repository and Archive, University of Zurich

ZORA URL: <https://doi.org/10.5167/uzh-18919>

Journal Article

Originally published at:

Vandesompele, J; Baudis, Michael; De Preter, K; Van Roy, N; Ambros, P; Bown, N; Brinkschmidt, C; Christiansen, H; Combaret, V; Lastowska, M; Nicholson, J; O'Meara, A; Plantaz, D; Stallings, R; Brichard, B; Van den Broecke, C; De Bie, S; De Paepe, A; Laureys, G; Speleman, F (2005). Unequivocal delineation of clinicogenetic subgroups and development of a new model for improved outcome prediction in neuroblastoma. *Journal of Clinical Oncology*, 23(10):2280-2299.

DOI: <https://doi.org/10.1200/JCO.2005.06.104>

From the Center for Medical Genetics, Department of Pathology, N. Goormaghtigh Institute for Pathology, Department of Pediatric Hematology and Oncology, Ghent University Hospital, Ghent; Department of Pediatric Hematology and Oncology, Cliniques St Luc, Université Catholique de Louvain, Brussels, Belgium; Department of Pathology, Stanford University Medical Center, Stanford, CA; Medizinische Klinik und Poliklinik V der Universität Heidelberg, Heidelberg; Gemeinschaftspraxis Pathologie, Am Fuchsengraben 3, Starnberg; Universitätskinderklinik, Marburg, Germany; Children's Cancer Research Institute, St Anna Kinderspital, Vienna, Austria; Institute of Human Genetics, University of Newcastle upon Tyne, Newcastle upon Tyne; Addenbrookes Hospital, Cambridge, United Kingdom; Centre d'Oncologie Génétique, Centre Léon Bérard, Lyon; Department of Pediatrics, University Hospital Center, Grenoble, France; Department of Oncology, Our Lady's Hospital for Sick Children, and National Centre for Medical Genetics, Our Lady's Hospital for Sick Children, Dublin, Ireland.

Submitted June 21, 2004; accepted December 30, 2004.

Supported by BOF-grant 011F1200 and 011B4300, GOA-grant 12051203, FWO-grant G.0028.00 and VEO-grant 011V1302. Katleen De Preter is an aspirant with the Fund for Scientific Research Flanders (FWO-Vlaanderen). Nadine Van Roy is a post-doctoral researcher with the FWO. Jo Vandesompele is supported by a post-doctoral grant from the Institute for the Promotion of Innovation by Science and Technology in Flanders (IWT).

Presented in part at the Advances in Neuroblastoma Research Meeting, Paris, France, June 17-19, 2002, and at the 8th European Workshop on Cytogenetics and Molecular Genetics of Human Solid Tumours, Barcelona, Spain, September 12-15, 2002.

This text presents research results of the Belgian program of Interuniversity Poles of Attraction initiated by the Belgian State, Prime Minister's Office, Science Policy Programming.

Authors' disclosures of potential conflicts of interest are found at the end of this article.

Address reprint requests to Jo Vandesompele, Center for Medical Genetics Ghent (CMGG), Ghent University Hospital, MRB, De Pintelaan 185, B-9000 Ghent, Belgium; e-mail: Joke.Vandesompele@UGent.be.

© 2005 by American Society of Clinical Oncology

0732-183X/05/2310-2280/\$20.00

DOI: 10.1200/JCO.2005.06.104

Unequivocal Delineation of Clinicogenetic Subgroups and Development of a New Model for Improved Outcome Prediction in Neuroblastoma

Jo Vandesompele, Michael Baudis, Katleen De Preter, Nadine Van Roy, Peter Ambros, Nick Bown, Christian Brinkschmidt, Holger Christiansen, Valérie Combaret, Maria Lastowska, James Nicholson, Anne O'Meara, Dominique Plantaz, Raymond Stallings, Bénédicte Brichard, Caroline Van den Broecke, Sylvia De Bie, Anne De Paepe, Geneviève Laureys, and Frank Speleman

A B S T R A C T

Purpose

Neuroblastoma is a genetically heterogeneous pediatric tumor with a remarkably variable clinical behavior ranging from widely disseminated disease to spontaneous regression. In this study, we aimed for comprehensive genetic subgroup discovery and assessment of independent prognostic markers based on genome-wide aberrations detected by comparative genomic hybridization (CGH).

Materials and Methods

Published CGH data from 231 primary untreated neuroblastomas were converted to a digitized format suitable for global data mining, subgroup discovery, and multivariate survival analyses.

Results

In contrast to previous reports, which included only a few genetic parameters, we present here for the first time a strategy that allows unbiased evaluation of all genetic imbalances detected by CGH. The presented approach firmly established the existence of three different clinicogenetic subgroups and indicated that chromosome 17 status and tumor stage were the only independent significant predictors for patient outcome. Important new findings were: (1) a normal chromosome 17 status as a delineator of a subgroup of presumed favorable-stage tumors with highly increased risk; (2) the recognition of a survivor signature conferring 100% 5-year survival for stage 1, 2, and 4S tumors presenting with whole chromosome 17 gain; and (3) the identification of 3p deletion as a hallmark of older age at diagnosis.

Conclusion

We propose a new regression model for improved patient outcome prediction, incorporating tumor stage, chromosome 17, and amplification/deletion status. These findings may prove highly valuable with respect to more reliable risk assessment, evaluation of clinical results, and optimization of current treatment protocols.

J Clin Oncol 23:2280-2299. © 2005 by American Society of Clinical Oncology

INTRODUCTION

Neuroblastoma is the most frequent extracranial solid tumor in children and originates from neural crest-derived sympathetic nerve cells. In contrast to many other pediatric malignancies, progress in treatment (especially for advanced-stage tumors) has been relatively modest. Hence, at

present, this tumor still poses a major challenge to the clinical oncologist. Although tumor stage and age at diagnosis are important predictors for patient outcome and are critical parameters for therapy stratification, a significant number of patients with apparently low-risk neuroblastoma at diagnosis relapse and require more aggressive treatment. Similarly, more than half of the

patients with adverse prognostic features at present cannot be cured, despite intensive multimodal therapy. In view of the unpredictable tumor behavior, many studies have aimed at the identification of additional factors for prognostic stratification.

Deletion of the short arm of chromosome 1, amplification of the *MYCN* proto-oncogene, and diploidy or tetraploidy were recognized quite early as genetic markers for aggressive neuroblastomas.¹⁻³ However, the overall picture of the different genomic changes in the various tumor stages remained incomplete for a long time. The importance of loss of chromosome regions other than 1p (ie, 2q, 3p, 4p, 9p, 11q, 14q, and 18q) was demonstrated by loss-of-heterozygosity studies.⁴⁻⁶ Losses of 3p, 9p, and 11q may also have prognostic value.⁷⁻¹⁰ A major landmark was the recognition of the high incidence of unbalanced 17q rearrangements by molecular cytogenetics, and the subsequent demonstration that the resulting partial 17q gain was the most powerful genetic predictor for poor outcome.^{11,12}

Many of the aforementioned studies focused on one or a few particular chromosomal regions. Hence, a comprehensive overview of the occurrence of the previously mentioned imbalances and their interrelationship could not be obtained. As successful karyotyping was not possible for a high proportion of neuroblastomas, it was not until the introduction of comparative genomic hybridization (CGH) that screening for DNA copy number gains and losses across the entire genome became feasible.^{13,14} This approach indeed proved to be particularly useful to address this issue, and consequently led to more general insights into the genetic heterogeneity of this enigmatic childhood tumor.¹⁵⁻²¹ Among others, evidence was obtained for a new genetic subgroup of *MYCN* single-copy neuroblastomas, characterized by loss of 11q, often in association with loss of 3p.^{15,20,21}

Despite these significant new findings, published CGH data formats for representation of gains and losses (either ideogram or International System for Human Cytogenetic Nomenclature [ISCN] description) do not allow in-depth analysis of large series of tumors. Here we illustrate the use of an available online tool for conversion of conventional CGH data into a digitized format (a band-specific aberration matrix) amenable for a more comprehensive genetic subgroup discovery. Global data mining and multivariate survival analyses on 231 published CGH results from neuroblastoma tumors firmly established the existence of three major clinicogenetic subgroups in neuroblastoma and provided to be a comprehensive assessment of prognostic parameters with independent power, leading to identification of a survivor signature for neuroblastoma and a new mathematical model for improved outcome prediction.

MATERIALS AND METHODS

Tumor Samples

Previously published CGH data on primary neuroblastoma tumors were included in this study based on the availability of

both individual band-specific CGH results for each tumor, as well as clinical patient information (stage, age at diagnosis, progression, and survival status). Samples without genetic aberration were excluded. This yielded a compilation of 231 unique cases from eight publications,¹⁵⁻²² of which 195 were also part of another multicenter study on 313 cases.¹¹ In this previous study, the consistency of the CGH data among five European centers (from which the majority of the cases in this study originate) was assessed, and no significant differences between laboratories were detected. Each referenced study has properly validated their CGH methodology and results. Where possible, clinical information was updated with respect to the original publication. All CGH aberration data can be accessed through the public Progenetix repository,²³ under ICD-O-3 (International Classification of Diseases for Oncology) code 9500/3. The sample identifiers from the Progenetix neuroblastoma case table are identical to those in the Supplemental Table (available online only in the full-text version; it is not included in the PDF [via Adobe® Acrobat Reader®] version), and are linked to the original publication (PubMed number) and CGH aberration pattern. Tumor stage was defined according to the International Neuroblastoma Staging System,²⁴ and risk status, according to the International Neuroblastoma Pathology Classification.²⁵ Event-free survival was defined as the time between initial diagnosis and relapse or death, or time between diagnosis and last follow-up if no event had occurred. The patients were treated according to the national protocols adapted to age and stage in use at that time in their country. Stratified survival analyses indicated that there were no significant differences in patient outcome in the various countries, considering either all patients together, or only the stage 4 tumors, or only infants (for these three groups, sufficient samples were available for reliable analysis; data not shown). The introduction of more homogeneous treatment regimens through the recently created International Society of Pediatric Oncology (SIOP)–Europe Neuroblastoma Group will allow confirmation of our results in a prospective study.

CGH Data Conversion

The ISCN2matrix converter at Progenetix²³ was used for both online conversion of the chromosome aberration list in ISCN format to a band-specific aberration matrix, as well as generation of a band-specific graphical representation of chromosomal gains and losses. During the conversion process, the CGH-based ISCN reverse in situ hybridization annotated karyotype (Supplemental Table) is resolved into 393 chromosome bands with categorical variables indicating the aberration status (−1: loss; 0: normal; +1: gain; +2: amplification), resulting in an average size of 7.9 megabases per annotation unit (band), well in the range of the spatial resolution achieved by chromosomal CGH.²⁶

Exploratory Data Mining and Statistical Analysis

The J-Express version 2.1 package²⁷ was used for exploratory data mining, such as principal component analysis (PCA) and hierarchical clustering. PCA is a mathematical procedure to reduce the dimensionality of the data by transforming a high number of (possibly) correlated variables (ie, chromosome bands) into a (smaller) number of uncorrelated (independent) variables called principal components. The first principal component accounts for as much of the variability in the data as possible, and each succeeding component accounts for as much of the remaining variability as possible. Mapping of the original variables onto the first two or three principal components (in a 2-D or 3-D plot, respectively)

provides a way to detect structure in the data and to classify variables. Cluster analysis is a technique used for combining variables (ie, chromosome bands or tumor samples) into groups or clusters, based on their similarity. Different (dis)similarity measures and clustering algorithms have been tested, and all brought about equivalent results (a representative example is shown using average linkage [unweighted pair group method with arithmetic mean] and standard correlation as similarity metric). Holzman and Kolker²⁸ provide detailed information on explorative data mining techniques (citing several good books that cover this topic). Statistical analyses were performed with SPSS version 11 (SPSS Inc, Chicago, IL). Descriptive statistics based on χ^2 tests were used to address the distribution of the genetic and clinical parameters, and the International Neuroblastoma Pathology Classification (INPC) risk status in the three tumor clusters, or to demonstrate the significant correlation between two parameters. The Kaplan-Meier univariate survival analysis method and log-rank test were used to estimate overall survival and event-free survival. A stepwise Cox proportional hazards model (successive exclusion of nonsignificant covariates with $P > .05$) was applied to test the independent significant influence of different genetic and clinical parameters on patient outcome. Verification of the proportional hazards assumption (stating that a particular covariate should be proportionally related to the baseline hazard) was done by inspecting the log-minus-log plot of the survival function. Nonparametric Mann-Whitney testing was used to compare the age at diagnosis between the different genetic subgroups.

Definition of Genetic Aberrations in Statistical Analyses

The chromosome 17 status was defined as partial chromosome 17q gain (unbalanced gain of 17q relative to 17p), whole chromosome 17 gain (an entire extra chromosome 17 relative to ploidy), or normal (no gain of chromosome 17q material relative to ploidy). Chromosome 1q gain was defined as partial 1q gain relative to ploidy (irrespective of chromosome 1p status). The term "deletion" was only used for tumor samples with partial loss of a chromosome (eg, 11q deletion, in contrast to whole chromosome 11 loss). A normal chromosome arm status therefore indicated absence of deletion (either no aberration or a numerical change). The presence of either one of the following three genetic defects (*MYCN* amplification or deletion of 1p or 11q) is referred to as a positive amplification/deletion status (as opposed to a negative amplification/deletion status, indicating a *MYCN* single copy number and intact chromosomes 1 and 11).

RESULTS

Explorative and statistical analyses were applied to whole genome chromosome status aberration information obtained by CGH of 231 primary untreated neuroblastoma tumors (see Materials and Methods). The median age at time of diagnosis of these patients was 19.0 months. The median follow-up time for survivors was 42.8 months (interquartile range, 20.0 to 70.8). Of the 231 tumors, 88 were from infants younger than 1 year, and 143 were from children older than 1 year. According to the criteria of the International Neuroblastoma Staging System, 32 tumors

were classified as stage 1, 35 as stage 2, 31 as stage 3, 100 as stage 4, and 33 as stage 4S.

Generation of a Band-Specific Aberration Matrix

For all selected cases, the aberrations identified by CGH were described according to the ISCN (ISCN 1995) guidelines and were combined with patient follow-up, age at time of diagnosis, tumor stage, ploidy, and INPC risk status information (Supplemental Table). The CGH-based reverse in situ hybridization-annotated karyotype information was parsed with the ISCN2matrix converter to a 393-band aberration matrix suitable for further data mining, containing the aberration status (lost, gained, amplified, or normal) for each individual chromosome band.

Visualization of Independent Genetic Events by PCA

A key feature of our proposed strategy for exploratory CGH data mining is the identification of the relevant and independent genetic events before further analysis. This is of major importance, as different chromosome bands in the generated aberration matrix do not represent independent variables: there is a high probability that neighboring bands display the same aberration status because they are linked to the same genetic defect (or normal status). As a result, genetic defects involving more bands have a higher weight in pattern discovery. Therefore, the predominant pattern will be dictated by the chromosome(s) (arms) containing the highest number of bands (for example, see the clustering of the neuroblastoma cases on the Progenetix²³ Web site, where chromosome 7 clearly has the highest weight). In contrast, genetic defects represent independent single events and should have equal weight, irrespective of the number of bands involved in the particular aberration.

To achieve this goal, we applied PCA to the 393-band aberration matrix for the 231 tumor samples. On projection of the 393 chromosome bands on the first two principal components, a clear picture of the chromosomal changes in neuroblastoma tumorigenesis emerges, with losses in the bottom left part, and gains in the upper right part of the projection (Fig 1). The PCA algorithm succeeds in grouping bands from the same chromosome or chromosome arm together, solely based on the aberration status of each band in the panel of tumors. It is also apparent from Figure 1 that some chromosomes are split into one or more band clusters, indicating that different regions in these chromosomes display different aberrations patterns in the tumor panel. In keeping with the PCA method, bands that cluster further away from the origin explain more variance and therefore represent significant alterations (eg, 2p23pter amplification, 17q gain, and loss of 1p and 11q). In contrast, bands closer to the center are not frequently altered in neuroblastoma.

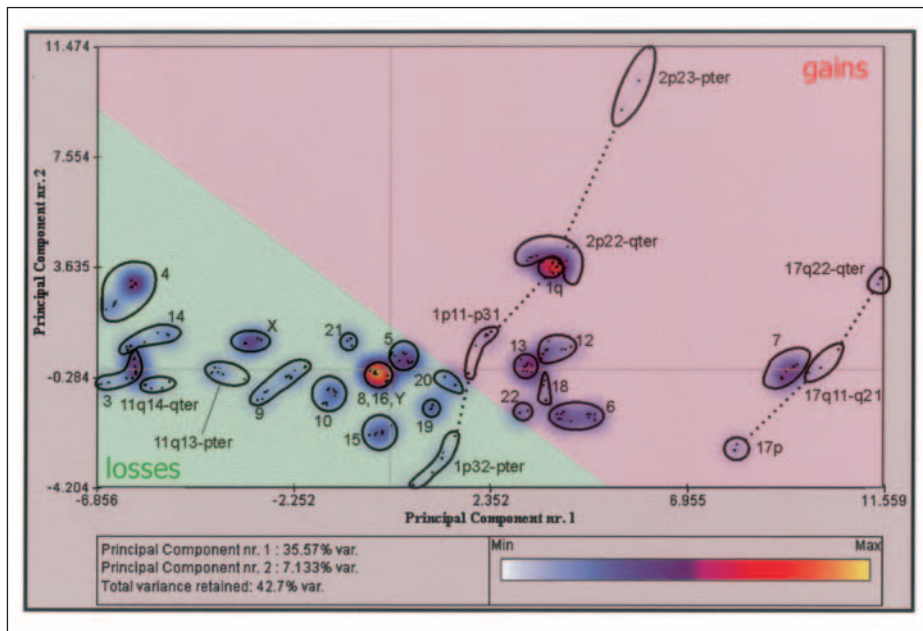


Fig 1. Principal component analysis of copy number information for 393 chromosome bands in 231 neuroblastoma tumors. Projection of the chromosome bands on the first two principal components (explaining 42.7% variance) delineates chromosomal regions that are relevant to neuroblastoma tumorigenesis.

Hierarchical Cluster Analysis

From each band cluster in the PCA projection, one band was selected to represent this chromosomal region. If all bands from a single chromosome (except acrocentric chromosomes) were grouped into one cluster, two bands per chromosome were selected (one from each arm) to exclude the possibility that a smaller proportion of tumors could not be discriminated based on a possible differential aberration status for the short and long arms. Accordingly, the 393-band aberration matrix was reduced to a 45-band matrix, representing independent variables. Hierarchical clustering using different similarity or distance measures and clustering algorithms yielded a series of equivalent aberration patterns with three recurring distinct tumor clusters. A representative example, including visualization of the individual clusters on separate ideogram charts, is shown in Figures 2A and B.

Cluster 1 contains 94 tumors with predominantly numerical aberrations (typical gains of chromosomes 6, 7, and 17, and losses of chromosomes 3, 4, 11, and 14). The other clusters are both characterized by structural chromosome aberrations, such as partial 17q gain, 11q deletion, and to a lesser extent, 3p deletion in the 45 cases of cluster 2; and partial 17q gain, *MYCN* amplification, 1p deletion, and to a lesser extent, 1q gain in the 74 cases from cluster 3. More than 92% of all tumors fall into these three genetic subgroups. The remaining tumors are mainly characterized by absence of recurrent genetic aberrations.

Genetic Subgroups in Relation to Clinical Variables

Table 1 presents the relationship between clinical, genetic, and histopathologic features and the three major

genetic subgroups as evidenced from hierarchical cluster analysis. Tumor stage (1, 2, and 4S combined v 3 or 4); age at time of diagnosis; ploidy; INPC risk status; *MYCN* copy number; and chromosome 1p, 1q, 3p, 11q, and 17q status are significantly nonrandomly distributed in the three clusters ($P = .039$ to $P < .0001$). For none of the other regions for which frequent loss has been reported (4p, 9p, 14q, 16p, or 18q) could a significant association be demonstrated with any of the clusters ($P > .1$).

While patients from cluster 1 are clearly diagnosed at a younger age compared with patients from cluster 2 or 3 ($P < .0001$), there is also a significant difference between clusters 2 and 3 ($P = .0078$; Table 2). The cases with 3p deletion seem to be partially responsible for the older age at diagnosis in cluster 2, as within this cluster, tumors with loss of 3p have a older age at diagnosis compared with 3p-intact cases (median age, 60.5 v 39.0 months; $P = .027$).

In keeping with the previously mentioned nonrandom distribution of several parameters within the three genetic subgroups, the Kaplan-Meier overall survival estimates are significantly different between clusters 1 and 2 or clusters 1 and 3 ($P < .0001$), while no difference was found between clusters 2 and 3 ($P = .62$; Fig 2C).

Univariate Survival Analysis

To determine which parameters contribute to prognosis, we first tested each variable in a univariate Kaplan-Meier survival analysis of all 231 patients (Table 3; Figs 3A and B). Tumor stage, age at diagnosis, ploidy, INPC risk status, *MYCN* gene copy number, and chromosome 1p, 1q, 11q, and 17q status are all significantly associated with overall and (most often also) event-free survival.

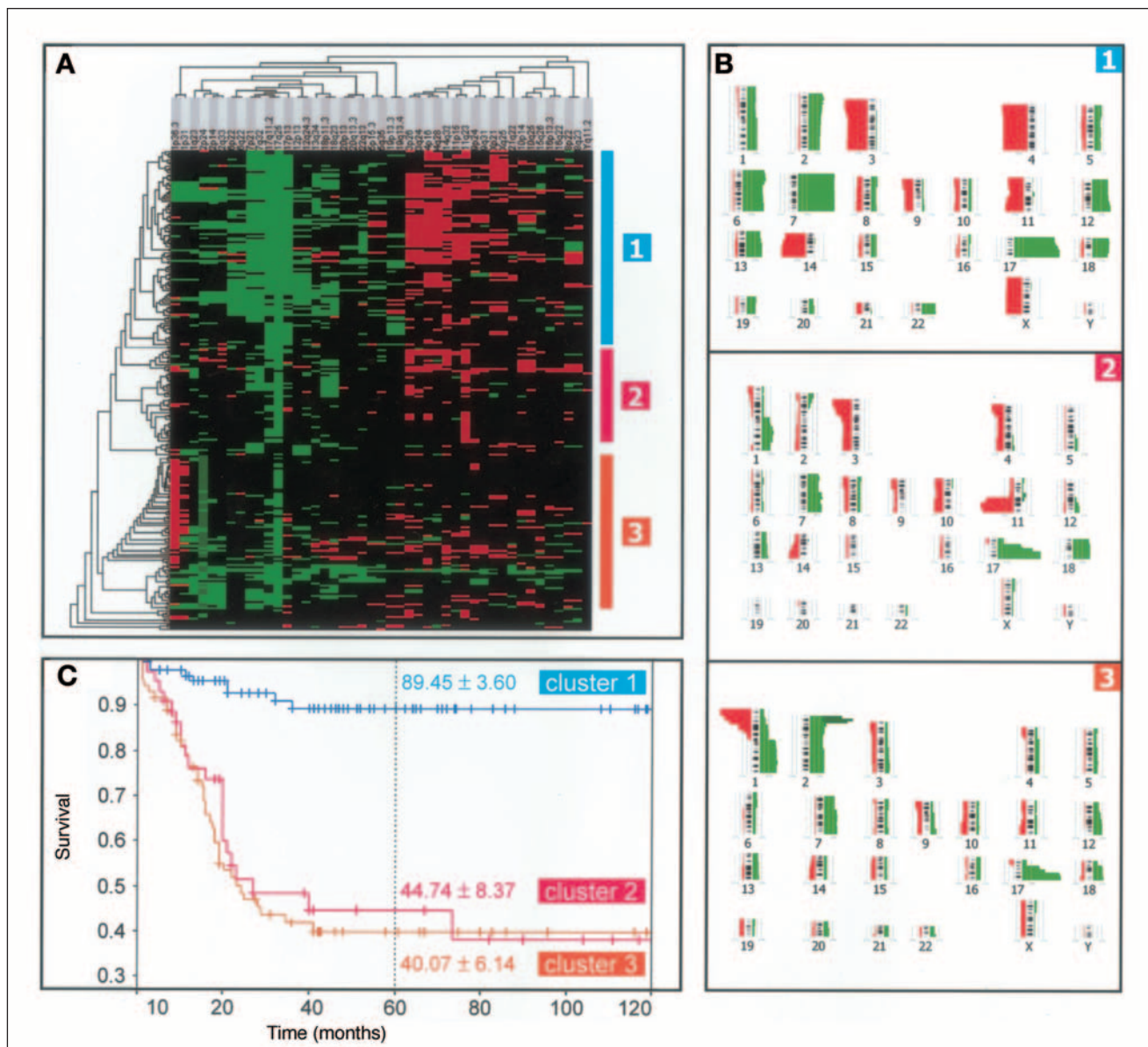


Fig 2. Delineation of three distinct clinicogenetic subgroups by (A) hierarchical clustering (green: gain; red: loss; dark green: amplification); (B) ideogram-based representation of chromosomal gains and losses (same color legend as in A); and (C) Kaplan-Meier overall survival analysis (5-year estimates \pm SE, in months).

Besides confirmation of known significant parameters in univariate survival analysis, this study demonstrated for the first time that a normal chromosome 17 status is associated with a poor prognosis. Losses of 3p, as well as losses of other regions (4p, 9p, 14q, 16p, or 18q) have no predictive power ($P > .1$; data not shown).

Multivariate Survival Analysis

To identify which parameters that showed significant predictive power in univariate analysis are independently correlated to patient outcome, an initial stepwise Cox proportional hazards procedure was applied to all 231 cases incorporating clinical and genetic parameters that were

available for all samples. Age and the status of *MYCN*, 1p, 1q, and 11q were excluded from the final model of overall survival probability ($P = .81$, $P = .38$, $P = .11$, $P = .14$, and $P = .87$, respectively). The remaining predictors for adverse outcome were tumor stage 3 (hazard ratio, 2.66; 95% CI, 1.05 to 6.74; $P = .039$), tumor stage 4 (hazard ratio, 4.63; 95% CI, 2.06 to 10.38; $P = .00020$), normal chromosome 17 status (hazard ratio, 3.19; 95% CI, 1.22 to 8.32; $P = .018$), and partial 17q gain (hazard ratio, 3.82; 95% CI, 1.64 to 8.90; $P = .0019$).

When the Cox proportional hazards procedure was applied to model event-free survival probability, only a normal

Table 1. Distribution of Clinical, Genetic, and Histopathologic Parameters in the Three Clinicogenetic Subgroups

Parameters	Cluster 1		Cluster 2		Cluster 3		P*
	No. of Patients	% Within Each Cluster	No. of Patients	% Within Each Cluster	No. of Patients	% Within Each Cluster	
Tumor stage							
1, 2, 4S	72	77	7	16	14	19	< .0001
3	13	14	2	4	16	22	
4	9	9	36	80	44	59	
Age, years							
< 1	60	64	5	11	19	26	< .0001
≥ 1	34	36	40	89	55	74	
MYCN gene							
Single copy	94	100	45	100	23	31	< .0001
Amplified	0	0	0	0	51	69	
Chromosome 1p							
Normal	90	96	40	89	23	31	< .0001
Deleted	4	4	5	11	51	69	
Chromosome 1q							
Normal	89	95	35	78	52	70	.00012
Gain	5	5	10	22	22	30	
Chromosome 3p							
Normal	87	93	33	73	70	95	.00053
Deleted	7	7	12	27	4	5	
Chromosome 11q							
Normal	85	90	15	33	68	92	< .0001
Deleted	9	10	30	67	6	8	
Chromosome 17q							
Normal	0	0	2	4	11	15	< .0001
Whole chromosome gain	84	89	6	13	7	9	
Partial 17q gain	10	11	37	82	56	76	
Ploidy†							
Near-triploid	21	68	2	33	0	0	< .0001
Near-diploid/tetraploid	10	32	4	67	19	100	
INPC risk status‡							
Favorable	11	33	1	11	3	10	.039
Unfavorable	22	67	8	89	26	90	

*P values calculated with the χ^2 test.
 †Not available for all cases.

chromosome 17 status (hazard ratio, 4.80; 95% CI, 2.39 to 9.61; $P < .0001$) and partial chromosome 17q gain (hazard ratio, 5.66; 95% CI, 3.26 to 9.82; $P < .0001$) remained independent significant predictors for adverse prognosis.

Table 2. Age at Time of Diagnosis

Cluster	No. of Patients	Mean Age	Median Age	Interquartile Range	P*
1	94	14.3	9.0	4.0-16.3	
2	45	47.2	41.0	26.4-62.5	
3	74	34.4	26.0	11.0-52.0	
Comparison					
1 v 2					.0001
1 v 3					.0001
2 v 3					.0078

NOTE. Age is given in months.
 *Mann-Whitney two-independent-samples test.

No Cox regression model could be tested taking both INPC risk status and ploidy into account, as only 18 cases for which both these parameters were determined were available. When tested separately (in conjunction with the other clinical and genetic parameters), ploidy had no independent predictive value, while the INPC risk status showed only marginal significance ($P = .12$ for retention and $P = .046$ for removal of this parameter in the model). Please note that these conclusions should be handled with care, as ploidy and INPC information was available for only 26% and 33% of the cases, respectively.

Stratified Survival Analyses for Chromosome 17 Status or Tumor Stage

Multivariate analysis indicated that chromosome 17 status and tumor stage are the only significant independent single parameters to model patient outcome. To determine which parameters further contribute to survival within

Table 3. Univariate Kaplan-Meier Survival Estimates

Parameters	No. of Patients	5-Year OS		OS <i>P</i> *	5-Year EFS		EFS <i>P</i> *
		OS	SE		EFS	SE	
Tumor stage							
1, 2, 4S	100	92.32	2.80		72.25	5.08	
3	31	63.62	9.31	.0003	49.22	11.12	.058
4	100	30.73	5.28	< .0001	27.81	5.10	< .0001
Age							
< 1	88	85.55	4.12		70.55	5.74	
≥ 1	143	46.87	4.67	< .0001	37.00	4.68	< .0001
MYCN gene							
Single copy	180	68.97	3.86		55.77	4.41	
Amplified	51	36.69	7.29	< .0001	31.20	6.95	.0008
Chromosome 1p							
Normal	167	70.35	3.98		58.12	4.57	
Deleted	64	39.36	6.66	< .0001	29.64	6.51	< .0001
Chromosome 1q							
Normal	190	67.30	3.73		56.62	4.14	
Gain	41	37.53	8.21	.0013	24.39	7.71	.0018
Chromosome 3p							
Normal	205	62.97	3.75		51.77	4.07	
Deleted	26	52.50	10.48	.21	37.27	10.35	.14
Chromosome 11q							
Normal	182	66.10	3.88		55.56	4.17	
Deleted	49	44.83	8.04	.0055	29.91	8.43	.022
Chromosome 17q							
Whole chromosome gain	97	89.96	3.42		80.39	4.56	
Normal	27	56.30	10.33	< .0001	33.63	10.98	< .0001
Partial 17q gain	107	38.07	5.27	< .0001	26.36	5.36	< .0001
Ploidy							
Near-triploid	24	95.83	4.08		61.00	11.37	
Near-diploid/tetraploid	37	61.00	8.63	.018	50.91	8.66	.24
INPC risk status							
Favorable	15	93.33	6.44		77.04	11.97	
Unfavorable	62	55.96	7.03	.013	42.57	7.70	.036

Abbreviations: OS, overall survival; EFS, event-free survival.

*Log-rank statistic, for each variable with respect to the first variable (eg, stage 3 v stages 1, 2, and 4S).

specific subgroups, we performed stratified subgroup analyses (Table 4; Figs 4A to D).

Within the favorable-stage tumors (1, 2, or 4S), the following parameters were associated with lower overall survival probability (P values < 0.0001): *MYCN* amplification, 1p deletion, normal chromosome 17 status, and partial 17q gain. Again, it is important to note that both a normal chromosome 17 status as well as a partial 17q gain identify low-stage patients with increased risk. Patients with a low-stage tumor displaying whole chromosome 17 gain have a 100% survival probability (Fig 4C). For stage 3 or 4 tumors, no further significant parameters could be discriminated.

Within the group of patients whose tumor showed whole chromosome 17 gain, the following parameters were associated with lower overall survival: 11q loss ($P = .0019$), 1q gain ($P = .046$), age older than 1 year at diagnosis ($P < .0001$), and tumor stage 3 ($P < .0001$) and stage 4

($P < .0001$). In line with the stage-stratified survival estimates, patients with whole chromosome 17 gain diagnosed prior to age 1 year (62 of 97 patients) or with tumors belonging to stages 1, 2, or 4S (76 of 97 patients) displayed a 100% overall survival (Figs 4A and B).

Within the group of patients whose tumors showed a normal chromosome 17 status (in a background of other genetic defects), borderline significant association with adverse outcome could be demonstrated for 1q gain or 1p deletion ($P = .039$ and $P = .032$, respectively). Within the subgroup of high-risk tumors with partial 17q gain, only stage 4 had additional predictive power ($P = .022$; Fig 4D).

As the *MYCN* status is currently the only genetic parameter that is incorporated in therapy stratification, we tested whether the chromosome 17 status allowed further stratification in the group of *MYCN*-amplified and single-copy tumors. A normal chromosome 17 status or a partial 17q gain are both significantly associated with decreased

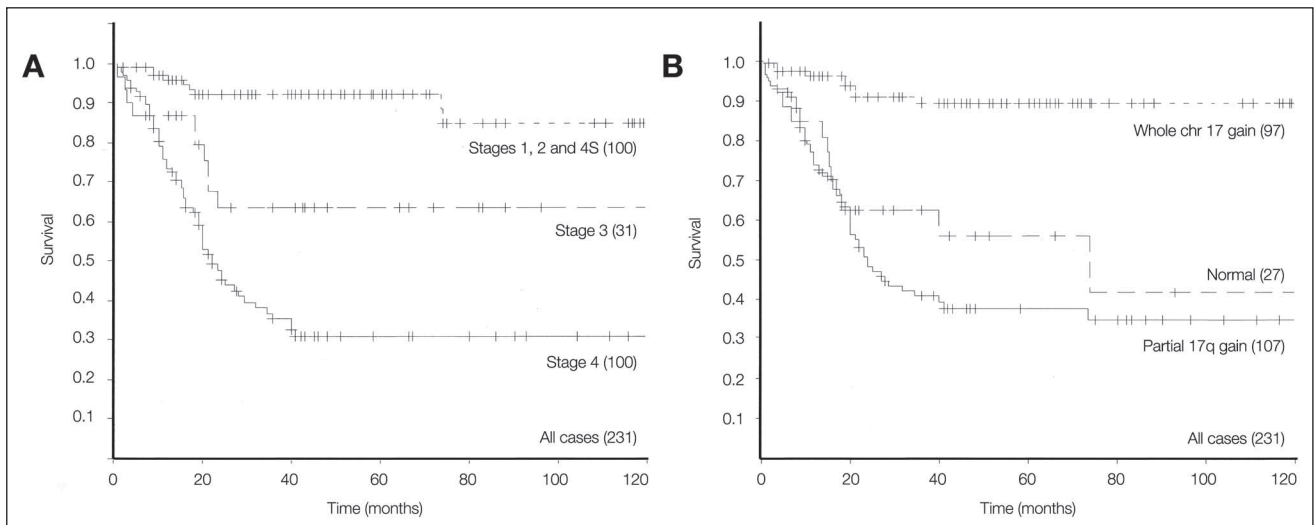


Fig 3. Kaplan-Meier overall survival analysis (in months) of all cases divided by tumor stage (A) or chromosome 17 status (B) (Table 3).

survival probability ($P < .001$) of patients with a *MYCN* nonamplified neuroblastoma. In contrast, chromosome 17 status allows no further stratification in *MYCN*-amplified tumors because *MYCN* amplification is almost invariably associated with a normal chromosome 17 or partial chromosome 17q gain status (there is only one tumor with *MYCN*-amplification in combination with whole chromosome 17 gain).

Development of a New Regression Model to Predict Outcome in Neuroblastoma

In the previous paragraphs, all patterns for chromosome 17 are considered as separate entities (whole chromosome gain, partial 17q gain, and a normal status), whereby it is demonstrated that a normal chromosome 17 status (just like partial 17q gain) is a significant predictor for poor outcome. However, up till now, no other study has considered neuroblastoma with normal chromosome 17 status as a separate entity. Most studies determined whether the tumor showed partial chromosome 17 gain or not (hence grouping together whole chromosome gain and a normal chromosome 17 status, hereafter referred to as “conventional dichotomization”). Because the fraction of tumors with a normal chromosome 17 status is relatively low (approximately 12% in the present study), conventional dichotomization still results in a highly significant association of chromosome 17 status with survival probability. Here, we propose a new improved dichotomization, whereby tumors with a normal chromosome 17 status are grouped together with those characterized by a partial 17q gain, and, as such, are compared as one entity with tumors with whole chromosome 17 gain. Cox proportional hazards regression not only demonstrated a greater relative risk ratio for the improved versus conventional dichotomization (8.56 ν 4.55), but also indicated that when both dichotomization

strategies were analyzed together, only the improved one retained independent predictive power.

The findings given in this section indicate that a whole chromosome 17 gain status confers a good prognosis and is the most important genetic parameter for a high survival probability. While whole chromosome 17 gain is strongly associated with a numerical aberration pattern, a normal chromosome 17 and partial 17q gain status are almost always found in a background of other structural chromosome aberrations. To test whether the structural aberration pattern itself (partial chromosome deletions or amplifications) is indicative of poor survival, we determined whether patients whose tumor showed any structural chromosome aberration had poorer outcomes compared with patients whose tumor presented with numerical aberrations only. As expected, a structural aberration pattern was a significant predictor in univariate survival analyses ($P < .0001$). Multivariate outcome prediction, however, could not attribute independent prognostic power to a structural aberration pattern. Further analyses indicated that a surprisingly high fraction of tumors with whole chromosome 17 gain (45 of 97 tumors) also displayed one or more structural aberrations (while it was expected that virtually all tumors [131 of 134] with a normal chromosome 17 status or partial 17q gain would show a structural aberration pattern). Closer inspection, however, revealed that only a minority of these cases (11 of 97) presented with one of the three genetic defects typically found in higher-stage aggressive tumors (found in clusters 2 and 3; ie, *MYCN* amplification, 1p deletion, or 11q deletion), suggesting that many of the structural defects observed in conjunction with whole chromosome 17 gain are nonfrequently occurring genetic changes. This prompted us to determine whether the presence of either *MYCN* amplification or loss of 1p or 11q

Table 4. Stratified Kaplan-Meier Survival Estimates

Stratum and Factors*	Patients		5-Year OS		OS P†
	No.	No. Dead	OS	SE	
Stage					
1, 2, 4S					
<i>MYCN</i>					
Single copy	93	5	96.34	2.08	
Amplification	7	4	42.86	18.70	< .0001
Chromosome 1p					
Normal	86	3	98.78	1.21	
Deleted	14	6	57.14	13.23	< .0001
Chromosome 17					
Whole chromosome gain	76	0	100.00		
Normal	8	4	41.67	20.48	< .0001
Partial gain	16	5	75.00	10.83	< .0001
3‡	31	11	63.62	9.31	
4‡	100	59	30.73	5.28	
Chromosome 17					
Whole chromosome gain					
Chromosome 11q					
Normal	89	5	92.61	3.23	
Deleted	8	3	62.50	17.12	.0019
Chromosome 1q					
Normal	91	6	91.98	3.20	
Gain	6	2	66.67	19.25	.046
Age at diagnosis, years					
< 1	62	0	100.00		
> 1	35	8	72.85	8.33	.0001
Stage					
1, 2, 4S	76	0	100.00		
3	11	3	70.71	14.29	< .0001
4	10	5	45.00	17.43	< .0001
Normal					
Chromosome 1q					
Normal	22	8	65.20	11.04	
Gain	5	4	20.00	17.89	.039
Chromosome 1p					
Normal	14	4	75.00	12.94	
Deleted	13	8	38.46	13.49	.032
Partial 17q gain					
Stages 1, 2, 4S	16	5	75.00	10.83	
Stage 3	16	7	55.68	13.74	.088
Stage 4	75	47	26.13	5.71	.022

Abbreviation: OS, overall survival.

*Listed are only those stratifying parameters with significant independent prognostic power according to multivariate regression (see Results), and only those factors with significant univariate predictive power in each stratum.

†Log-rank statistic for each factor variable with respect to the first variable (eg, normal chromosome 17 status v whole chromosome 17 gain).

‡No significant factors.

(hereafter referred to as a positive amplification/deletion status; see Materials and Methods) could serve as a new powerful and independent prognostic parameter. Indeed, Cox multivariate survival analysis indicated that the amplification/deletion status (hazard ratio, 2.04; 95% CI, 1.06 to 3.91; $P = .032$), the improved chromosome 17 status dichotomization (hazard ratio, 2.77; 95% CI, 1.14 to 6.72; $P = .025$), and tumor stage (3 and 4 v 1, 2, and 4S; hazard ratio, 3.49; 95% CI, 1.60 to 7.63; $P = .0017$) were independent predictors for adverse outcome. Table 5 gives an over-

view of the hazard ratios (relative to patients with a stage 1, 2, or 4S tumor showing whole chromosome 17 gain and a negative amplification/deletion status) for patients stratified according to previously mentioned independent outcome predictors. Subsequent confirmatory analyses indicated that the improved chromosome 17 status dichotomization indeed allowed further stratification in cases with a negative ($P < .0001$) or positive ($P = .052$) amplification/deletion status. Likewise, the amplification/deletion status parameter also allowed further stratification within the cases with

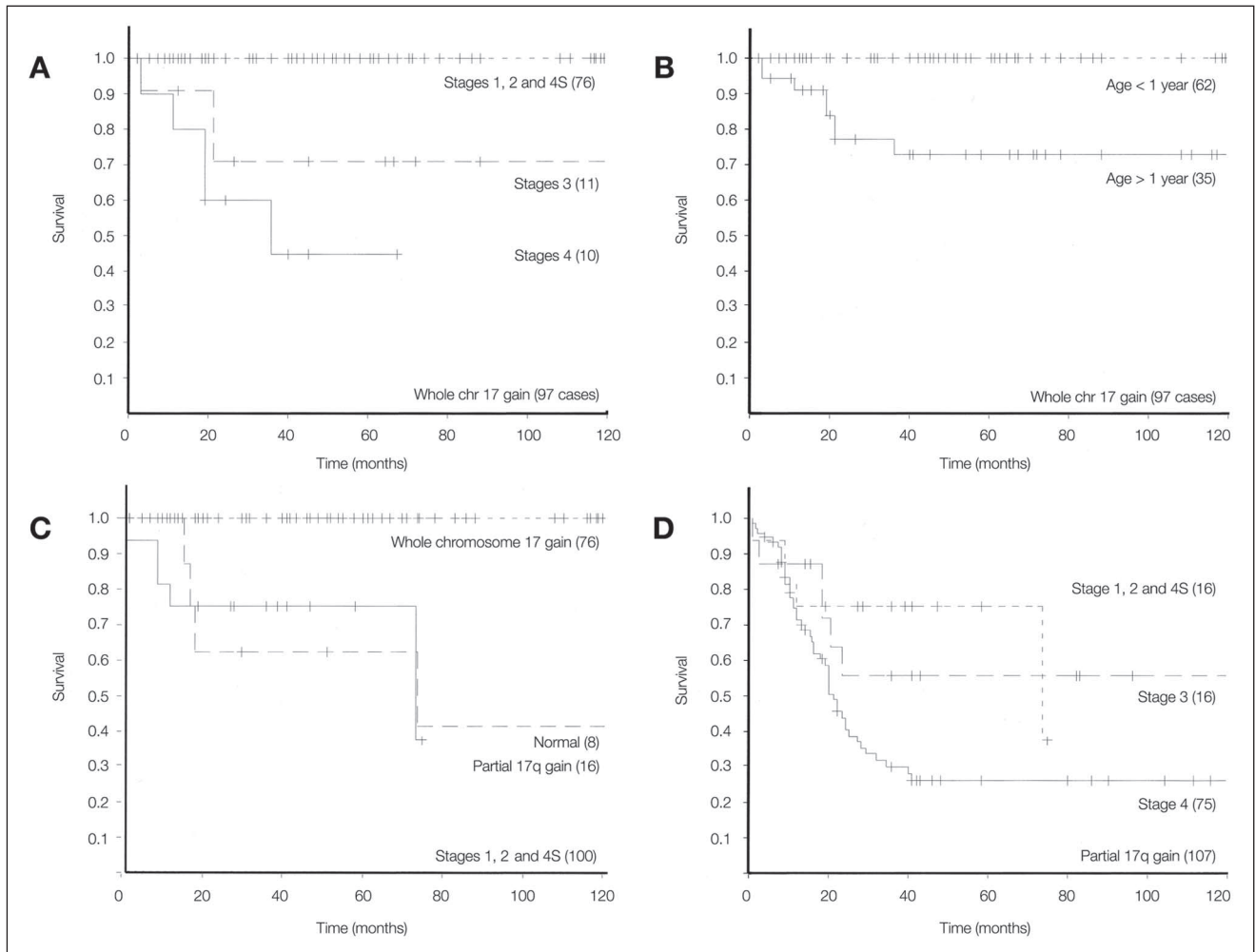


Fig 4. Stratified survival analysis of tumors presenting with whole chromosome (chr) 17 gain subdivided by (A) tumor stage or (B) age at diagnosis; (C) favorable-stage tumors subdivided by chromosome 17 status; or (D) tumors with partial 17q gain subdivided by tumor stage (Table 4).

whole chromosome 17 gain ($P = .024$), or either a normal chromosome 17 status or partial 17q gain ($P = .016$; Fig 5).

DISCUSSION

Deletion of the distal part of chromosome arm 1p and amplification of the *MYCN* oncogene were the first genetic markers of advanced-stage neuroblastoma recognized in the initial cytogenetic investigations of this tumor. Subsequently, an array of other recurrent structural chromosome aberrations was reported, and some were found to be associated with patient outcome. However, it was not until the advent of the whole genome scanning method CGH that a global view on the genetic heterogeneity and the interrelationship of the imbalances could be obtained. These studies not only provided insights in the genetic basis underlying the clinical variability associated with this childhood tumor, but most importantly, provided clues about the existence of

two different genetic subgroups of advanced-stage unfavorable neuroblastomas, characterized by *MYCN* amplification and loss of 11q, respectively.

Despite the wealth of information CGH brought about with respect to identification of chromosomal regions of consistent loss or gain, many publications suffer from a lack of uniform data presentation and detailed aberration information for the individual cases. As such, it has proven impracticable or impossible to reanalyze data or pool case results from different (often of relatively small sample size) studies to strengthen conclusions or gain further insight into the different aberration patterns or genetic subgroups that might exist. To overcome this problem, a public repository for published CGH data in a format suitable for data mining procedures has been initiated.²³ Equipped with the ability to convert analogous CGH profiles to a digitized data mining-compatible format, we sought to apply common bioinformatics algorithms to CGH-based chromosome

Table 5. Relative Risk Ratio for Neuroblastoma Patients Stratified for Stage, Chromosome 17, and Amplification/Deletion Status

	Whole Chromosome 17 Gain					Normal Chromosome 17 Status or Partial 17q Gain				
	No. of Patients	No. of Deceased	5-Year OS	SE	Hazard	No. of Patients	No. of Deceased	5-Year OS	SE	Hazard
Negative amplification/deletion status										
stages 1, 2, 4S	70	0	100		1.00	9	2	88.89	10.48	2.77
stages 3, 4	16	5	63.48	13.34	3.49	19	8	46.23	13.34	9.66
Positive amplification/deletion status										
stages 1, 2, 4S	6	0	100		2.04	15	7	60.00	12.65	5.64
stages 3, 4	5	3	40.00	21.91	7.12	91	54	32.48	5.53	19.68

Abbreviation: OS, overall survival.

aberration information, and performed for the first time a comprehensive and in-depth analysis of genetic aberrations occurring in the various neuroblastoma subtypes.

In the approach presented here, principal component analysis was an important step toward unbiased delineation

of independent genetic events before explorative and statistical analyses. Subsequent hierarchical clustering firmly established the existence of three distinct genetic subgroups. Interestingly, these three subgroups not only differ with respect to their genomic aberration patterns, but are also

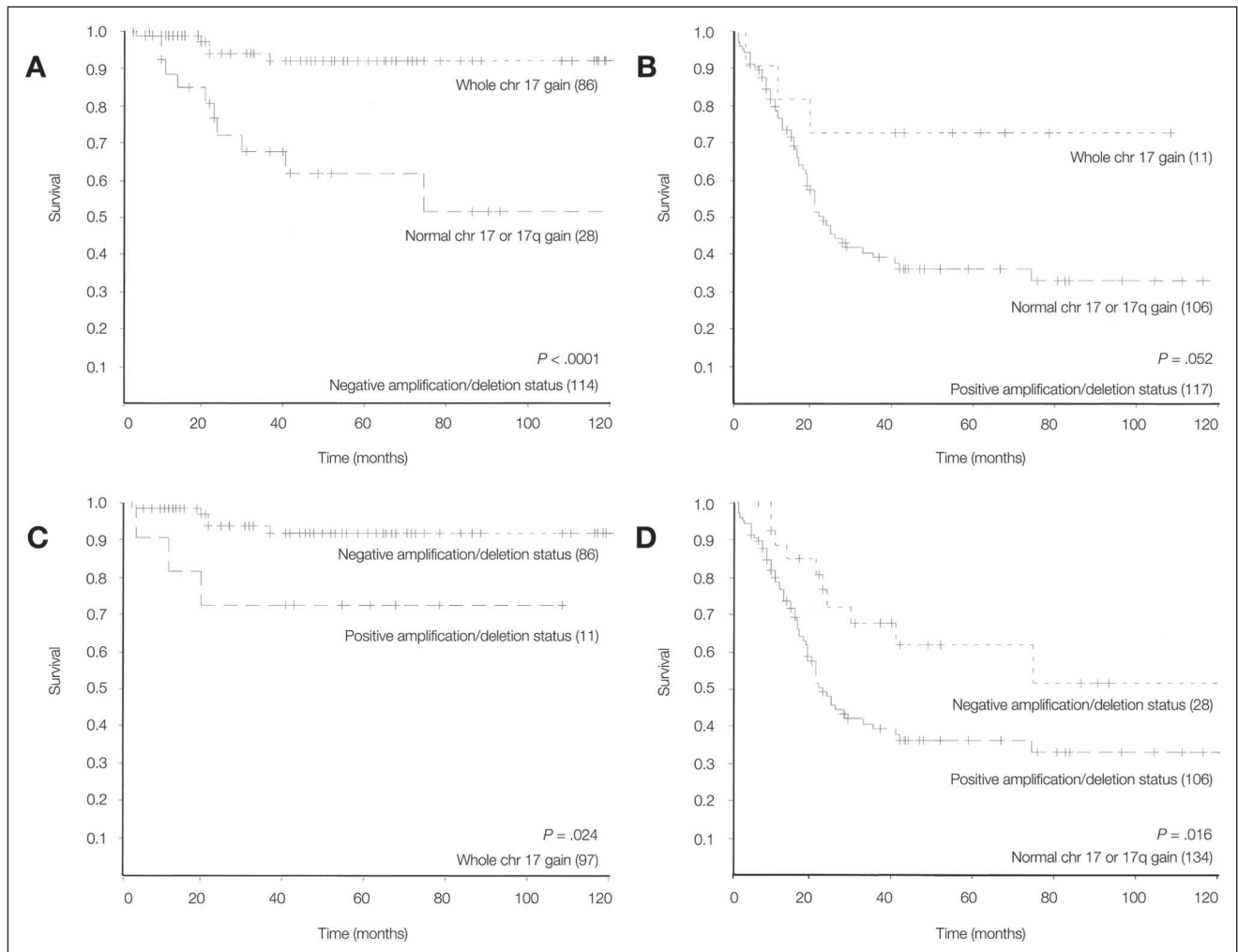


Fig 5. Stratified survival analysis of cases presenting with a negative (A) or positive (B) amplification/deletion status subdivided by chromosome (chr) 17 status; cases presenting with whole chromosome 17 gain (C) or normal chromosome 17 status/partial 17q gain (D) subdivided by amplification/deletion status.

characterized through significantly different age at time of diagnosis, tumor stage distribution, ploidy level, INPC risk status, and survival probability. Cluster 1 represents predominantly near-triploid low-stage tumors with numerical aberrations and favorable histology from infants (median age at diagnosis, 9 months) with excellent outcome. Cluster 2 contains predominantly near-diploid/tetraploid stage 4 tumors with unfavorable histology, partial 17q gain, and 11q loss, often in association with loss of 3p. These patients present with the oldest age at diagnosis (median age, 41 months) and have a poor overall 5-year survival of approximately 40%, which is similar to that of patients from cluster 3 (median age, 26 months), who present with near-diploid/tetraploid high stage tumors displaying unfavorable histology and partial 17q gain, loss of 1p, and *MYCN* amplification.

The difference in age at diagnosis between high-stage clusters 2 and 3 may be explained by a difference in growth rate and/or the need for an additional genetic defect in a cluster 2 tumor to become clinically manifest (as suggested by a large proportion of 3p loss in cluster 2, associated with an older age at diagnosis). This indicates that clusters 2 and 3 are clinically distinct and might behave differently, which suggests discrimination between those tumor subtypes in future therapeutic strategies.

While acknowledging the limitations of explorative cluster analysis (in that the answer is not absolute, and that different distance measures and cluster algorithms may result in differences between the generated patterns or clusters), we believe that the recurring patterns we observed, in addition to the significant nonrandom association of relevant neuroblastoma parameters to the observed clusters, render confidence to the presented clusters, delineating three major different clinicogenetic subgroups in neuroblastoma.

Although the existence of clinicogenetic subgroups has been proposed in previous studies, these conclusions were not based on in-depth analysis owing to various limitations such as sample size, tumor stage distribution, or noninclusion of all relevant genetic aberrations.^{5,10,20,29} In contrast, this study provides an unbiased and comprehensive assessment of the subgroups based on a large series of tumor samples belonging to all stages, and based on all relevant genetic, histopathologic, and clinical information. Furthermore, our finding of 3p loss as a hallmark of older age at diagnosis provides additional insight into the series of genetic events leading to a subtype of aggressive neuroblastoma.

To determine which of the individual parameters independently contribute to survival probability, stratified univariate and multivariate analyses were performed. Both analyses demonstrated that chromosome 17 status and tumor stage are the only significant independent predictors for patient outcome, corroborating previous studies^{11,29-31}

and emphasizing the need to include at least tumor stage and chromosome 17 status in future multivariate evaluations of prognostic parameters. As many of the cases in this article were also compiled in an even larger multicenter study (reporting only on chromosome 1 and 17, *MYCN* status, and ploidy), our conclusion about the prognostic significance of chromosome 17 is not surprising. However, more importantly, we obtained new information regarding patients with a normal chromosome 17 status. Please bear in mind that these tumors always displayed other cytogenetic aberrations (Supplemental Table), as we excluded tumors with no detectable changes (see Materials and Methods). We were able to demonstrate that a normal chromosome 17 status (in conjunction with other defects) is an independent marker, and that patients with these tumors had an equally adverse outcome compared with those with partial chromosome 17q gain, a finding that is particularly true for favorable-stage tumors 1, 2, and 4S. In other words, a normal chromosome 17 status or partial chromosome 17q gain identify a new subgroup of increased-risk patients with presumed favorable-stage tumors. This finding may have important clinical consequences with respect to proper treatment and assessment of new therapeutic protocols. It is important to note that we could not confirm the recently reported adverse prognostic power of 3p or 11q loss in localized and stage 4S tumors.³²

Taken together, these analyses indicate that the presence of an extra chromosome 17 (often in a background of other numerical aberrations) is the most important independent genetic indicator for excellent patient outcome, and suggest that these tumors represent a separate biologic entity of favorable neuroblastomas.

A second important new observation, in line with the previous statement, was the identification of a specific survivor signature for children with neuroblastoma. Within the subgroup of tumors with whole chromosome 17 gain, tumor stage and age at diagnosis seem to have additional predictive power: the group of patients with either a favorable-stage tumor (stages 1, 2, and 4S) showing whole chromosome 17 gain, or a tumor with whole chromosome 17 gain diagnosed before age 1 year, show a 100% overall survival (Fig 4). Considering that whole chromosome 17 gain is strongly associated with near-triploidy, the above findings are in keeping with the report that ploidy is a strong prognostic factor for children younger than 1 year at diagnosis.³

The fact that the *MYCN* status as a standard marker for neuroblastoma therapy stratification drops out of the multivariate analysis is not unexpected, nor contrary to published data. As in many other reports based on univariate analysis, *MYCN* amplification is also a strong predictor for adverse outcome in this study. However, when other genetic, clinical, or histopathologic parameters are taken into account (multivariate analysis), *MYCN* status no longer has independent predictive power, corroborating published

reports.^{11,29} This can be explained by the strong association of *MYCN*-amplification with other prognostic factors (eg, stage 4 and gain of 17q) that occur more frequently, and hence, can predict outcome for a larger proportion of patients. The fact that Cox proportional hazards modeling attributes independent prognostic value to those parameters that can predict an adverse outcome for as many patients as possible also explains why other genetic parameters that have univariate prognostic value (such as loss of 1p and 11q) drop out of the multivariate model when chromosome 17 status is included. This prompted us to investigate whether the combination of *MYCN* status and 1p or 11 deletion could serve as a new powerful independent predictor (besides chromosome 17 status) in multivariate survival analysis. Indeed, we could develop a new regression model that incorporates tumor stage (3 and 4 combined v 1, 2, and 4S); chromosome 17 status (whole chromosome gain v combined partial gain or normal chromosome status); and the combined status of *MYCN*, 1p, and 11q (amplification/deletion status). This new three-parametric model can predict patient outcome more accurately than any other tested model incorporating one or more of the available parameters (as evidenced by the relative risk ratio and overall score of the model). It will prove interesting to validate this model in other large cohorts of uniformly treated patients for whom all clinical, genetic, and histopathologic parameters are available. Again, the model demonstrates that in addition to the current incorporation of the *MYCN* status in therapy stratification, chromosome 17 status and preferably also chromosome 1 and 11 status should be routinely assessed and taken into consideration in the evaluation of clinical trials and possible future therapeutic stratifications.

While many studies have confirmed the initial report on the clinical significance of unbalanced 17q gain in neuroblastoma,¹¹ a recent fluorescence in-situ hybridization (FISH)-based study failed to attribute prognostic value to 17q gain.³³ Our observation that a normal chromosome 17 status is also a strong predictor for adverse outcome, and that in the referenced FISH study, conventional dichotomization is used (hence grouping together favorable tumors with whole chromosome 17 gain and unfavorable tumors with a normal chromosome 17 status) might (partly) explain why in this specific study, 17q gain was not recognized as a prognostic marker, especially if a relatively high proportion of cases with a true normal chromosome 17 status was included. The discrepant results might also be explained by the particular method that is used to score chromosome 17 gain. Most studies attributing

prognostic value to the chromosome 17 aberration status relied entirely or predominantly on CGH. The study that failed to confirm the chromosome 17 findings is based exclusively on FISH interpretation of 17q copy number gain. Preliminary data in our laboratory, based on FISH analyses, indicate large intratumoral heterogeneity of chromosome 17 copy numbers and aberration status (whole chromosome gain and partial gain present in the same tumor), complicating unequivocal interpretation. Multicolor interphase FISH and (microarray-based) CGH side-by-side comparisons are ongoing to assess concordance between these detection methods (data will be published elsewhere).

The present study is also relevant in light of current efforts of tumor subgroup classification based on transcriptome profiling using oligonucleotide or cDNA microarrays. These methods are relatively expensive and require significant amounts of high-quality RNA. Assessment of genetic defects at the DNA level with strong diagnostic and prognostic relevance may provide a valuable alternative, as demonstrated by other studies.³⁴⁻³⁷ In this context, the recent report indicating the superiority of genomic aberration patterns with respect to tumor subtype identification compared with expression profiles, is of particular interest.³⁸

Another important feature of our proposed scheme for data handling is its applicability to promising new whole genome profiling strategies such as Serial Analysis of Gene Expression-based digital karyotyping³⁹ and microarray-based CGH in which metaphases have been replaced by arrayed genomic BAC clones,^{40,41} cDNA transcripts,⁴² or oligonucleotides.^{43,44} These new technologies not only offer a significant increase in resolution, but are also adaptable to automation, leading to higher throughput. Hence, going from a cytogenetic to a molecular analysis level, it is expected that new aberrations will be identified, hopefully speeding up the discovery of molecular targets for the development of enhanced therapeutic approaches.

Acknowledgment

We gratefully acknowledge Jan Kohler and all other CGH collaborators for providing individual CGH profiles and updated clinical patient information. We also highly value the comments we received from the anonymous reviewers.

Authors' Disclosures of Potential Conflicts of Interest

The authors indicated no potential conflicts of interest.

Mining of Neuroblastoma CGH Data

Supplemental Table: Clinical, Genetic, and Histopathologic Parameters and CGH Aberrations for 231 Primary Untreated Neuroblastomas

Identifier	Cluster ^a	Stage	Age ^b	Event ^c	EFS ^d	Survival ^e	OS ^f	Ploidy ^g	INPC ^h	CGH Aberrations
NBL-Meta-1	1	4	95	1	32	1	32	—	U	rev ish enh(7p21p22, 7q21q36, 8p, 17q12q25) dim(2p24p25, 3p14p26, 4p, 11q14q25, X)
NBL-Meta-2	2	4	66	1	20	1	20	—	U	rev ish enh(1q22q25, 7q22, 7q32q36, 12q23q24, 17q12q25, 18) dim(9p13p24, 11q14q25, Y)
NBL-Meta-3	3	4	69	1	6	1	14	—	U	rev ish amp(2p23p24)
NBL-Meta-4	3	4	23	1	19	0	58	—	U	rev ish enh(2p12p22, 2p25, 17q11q25) dim(1p32p36) amp(2p23p24)
NBL-Meta-6	1	2	12	0	78	0	78	—	—	rev ish enh(7, 13, 17, 18) dim(3, 4p, 9p24q32, 11, 14, X)
NBL-Meta-7	3	4	14	0	58	0	58	—	F	rev ish enh(3q13q29, 17q11q25, 19p) dim(1p32p36, 15q11q13, 19q) amp(2p23p24)
NBL-Meta-8	1	2	5	0	55	0	55	—	F	rev ish enh(6p, 6q24q27, 7, 8p, 8q24, 17) dim(4, 14, 16q, X)
NBL-Meta-9	1	4S	6	0	54	0	54	—	F	rev ish enh(1p21q44, 2p25q21, 6p25q13, 6q24q27, 7, 12, 17, 22) dim(2q23q37, 3, 4, 5, 8, 10p13p15, 11p, 11q14q25, 14, 15q11q22, 18, 21, X)
NBL-Meta-11	1	1	4	0	49	0	49	—	F	rev ish enh(2, 7, 12, 17) dim(3, 4, 6, 8, 9p, 10, 11, 13, 14, 15, 18)
NBL-Meta-12	3	4	58	1	13	1	15	—	—	rev ish enh(1p31q44, 2p22q37, 2p25, 8q24, 17q11q25) dim(1p32p36, 3, 9, 11p12p14, 11q14q21, 13, 14, 15q11q15, 21q22) amp(2p23p24)
NBL-Meta-13	3	4	66	0	46	0	46	—	U	rev ish enh(17q11q25) dim(X) amp(2p23p24, 10p13p14, 10q24q25)
NBL-Meta-14	2	1	17	0	117	0	117	tri	U	rev ish enh(7, 8, 17, 18, X)
NBL-Meta-15	1	1	10	0	60	0	60	—	—	rev ish enh(6, 7, 8, 13, 17, 20, 22) dim(11, 12, 14)
NBL-Meta-16	2	1	36	0	67	0	67	tri	—	rev ish enh(1q, 5q23q35, 17) dim(2p23p25, 2q33q37, 3p21p26, 3q24q29, 4p15p16, 4q, 10q23q26, 11q14q25, 14q31q32)
NBL-Meta-17	1	1	12	0	71	0	71	di	U	rev ish enh(6, 7, 17, 19)
NBL-Meta-18	1	1	7	1	6	0	108	—	—	rev ish enh(7, 17, 19p) dim(9p)
NBL-Meta-19	1	1	0.1	0	119	0	119	—	—	rev ish enh(2, 6, 7, 12, 13, 17, 18)
NBL-Meta-21	1	2	11	0	88	0	88	tri	U	rev ish enh(2, 6, 7, 12, 17, 18, 22) dim(4, 9, 16, X)
NBL-Meta-22	1	2	3	0	54	0	54	—	—	rev ish enh(6, 9, 12, 17, 18, 20, 22) dim(4, X)
NBL-Meta-23	1	2	1	0	127	0	127	—	—	rev ish enh(6, 7, 17, 18p11q21, 19, 22) dim(3p22p26)
NBL-Meta-24	1	4S	3	0	108	0	108	—	F	rev ish enh(2p14p25, 17, 18p11q21, 19p13q13) dim(8q23q24, 11p14p15, 11q22q25, 14q32, 16q13q24)
NBL-Meta-25	4	4S	3	1	51	1	74	tri	U	rev ish enh(7, 18) dim(21, Xq22q28)
NBL-Meta-26	3	4	2	1	1.5	1	1.5	tetra	—	rev ish enh(2p22p25, 15q25q26, 17q22q25) dim(1p32p36, 9, 14q21q32, 19, 21q22, 22)
NBL-Meta-27	1	3	20	1	19	1	21	—	U	rev ish enh(1q, 12, 17, 19)
NBL-Meta-28	1	3	36	0	131	0	131	—	—	rev ish enh(16p, 17, 18p11q11, 19) dim(3p22p26, 3q26q29, 14)
NBL-Meta-29	1	3	8	0	66	0	66	tri	U	rev ish enh(6, 7, 8, 13, 17, 18) dim(14, 16q, X)
NBL-Meta-30	3	3	25	0	42.5	0	42.5	di	—	rev ish enh(12q13q24) dim(1p22p36) amp(2p23p24)
NBL-Meta-31	4	2	10	1	20	0	149	—	—	rev ish enh(5q14q22, 4q21q31) dim(14, 17p, 19, 22)
NBL-Meta-32	3	3	20	0	46	0	83	tetra	—	rev ish enh(2p23p24, 17q22q25) dim(1p22p36, 10)
NBL-Meta-33	3	4	101	1	19	1	19	—	U	rev ish enh(1q12q32, 2p23p25, 5q31q35, 6, 7, 11p, 13, 16p, 17, 18, 20, 21) dim(11q22q25)
NBL-Meta-34	2	4	31	1	8	0	111	—	—	rev ish enh(1q, 1p36, 5q31q35, 11q13, 12q21q24, 13, 17q) dim(3p22p26, 11q14q25, 14q22q32)
NBL-Meta-35	2	4	65	0	40	0	40	—	—	rev ish enh(7, 11q13, 17, 18) dim(3p14p26, 4p, 11q14q25, 20p)
NBL-Meta-37	1	4	47	1	24	1	36	—	—	rev ish enh(17, 19) dim(X)
NBL-Meta-38	3	4	57	1	24	1	25	di	U	rev ish enh(1q, 11q13, 17q, 7, 12) dim(1p, 11q14q25, 3, 10, 15) amp(2p23p24)
NBL-Meta-39	1	4	63	1	3	1	3	—	U	rev ish enh(2p11p15, 5p15q11, 12q22q24, 6, 7, 15, 16, 17, 18p11q21, 22) dim(2q, 4, 8, 9, 11p15q12, 11q14q25, 14, 21, X) amp(11q13)
NBL-Meta-40	2	4	57	1	13	1	21	di	U	rev ish enh(1q, 7p15p21, 17q) dim(2p23p25, 3p21p26, 11q14q23, 14q24q32)
NBL-Meta-41	2	4	49	1	15	1	20	—	—	rev ish enh(17q22q25) dim(1q42q44)
NBL-Meta-42	2	4	41	0	90	0	90	di	F	rev ish enh(17q21q25)
NBL-Meta-43	3	4	32	1	18	1	24	—	—	rev ish enh(2p, 17q22q25) dim(1p32p36, 3p14p26, 14q32, 17p, 18q22q23, 9)
NBL-Meta-44	3	4	17	0	116	0	116	tetra	—	rev ish enh(17q22q25) dim(1p33p36, 9p21p24) amp(2p23p24)
NBL-Meta-45	3	4	35	0	66	0	66	tetra	—	rev ish dim(1p31p36, 9p21p24) amp(2p23p24)
NBL-Meta-46	2	4	32	0	104	0	104	—	—	rev ish enh(1q23q32, 7q21q36, 17q22q25) dim(1q42q44, 5p, 8p, 10p, 11q14q25)

(continued on following page)

Supplemental Table: Clinical, Genetic, and Histopathologic Parameters and CGH Aberrations for 231 Primary Untreated Neuroblastomas (continued)

Identifier	Cluster ^a	Stage	Age ^b	Event ^c	EFS ^d	Survival ^e	OS ^f	Ploidy ^g	INPC ^h	CGH Aberrations
NBL-Meta-47	3	4	178	1	13	0	27.5	di	—	rev ish enh(1q32q44, 11q14q25, 22) dim(1p21p36, 3p22p26, 19q13) amp(2p23p24)
NBL-Meta-48	3	4	19	0	80	0	80	di	—	rev ish enh(2p25, 17q23q25) dim(1p31p36) amp(2p23p24)
NBL-Meta-49	3	4	33.5	0	86	0	86	di	—	rev ish enh(2p23p25, 2q22q37, 5q14q23, 17q, 18q12q23, 7, 12, 22q13)
NBL-Meta-51	1	1	4	1	8	0	11	—	—	rev ish enh(1, 2, 5p, 5q15q23, 6, 7, 12, 13q13q34, 17) dim(3, 4, 10, 11, 14, 15, 16)
NBL-Meta-52	1	1	17	0	5	0	5	—	—	rev ish enh(2p12p21, 2p23p25, 5, 7, 13, 17, 18) dim(3, 4, 14)
NBL-Meta-53	1	1	19	0	10	0	10	—	U	rev ish enh(6, 7, 13q21q34, 17, 18, 22) dim(3p21p26, 4, 10, 14q12q32, 15q21q26, 21)
NBL-Meta-54	2	1	9	0	9	0	9	—	U	rev ish enh(1p, 17, 18) dim(4, 8, 10, 14)
NBL-Meta-55	1	1	4	0	12	0	12	—	U	rev ish enh(7, 12, 17) dim(4, 21)
NBL-Meta-56	1	1	15	0	15	0	15	—	—	rev ish enh(5, 6, 7, 12, 17, 18q) dim(3, 4, 14, 22)
NBL-Meta-57	1	1	10	0	11	0	11	—	—	rev ish enh(1, 2, 5, 7, 12, 17, 19, 20, 22) dim(3, 4, 6, 8, 13, 14, 15q21q26, 18, 21)
NBL-Meta-58	1	2	26	0	21	0	21	—	U	rev ish enh(7, 13, 17, 18) dim(4)
NBL-Meta-59	3	3	96	0	14	0	14	—	U	rev ish enh(1q21q44, 2p23q37, 17q23q25, 18) dim(1p22p36, 3) amp(2p24p25)
NBL-Meta-60	1	3	11	0	15	0	15	—	U	rev ish enh(7, 17q22q25) dim(4, 11q22q25)
NBL-Meta-61	3	3	31	1	9	0	43	—	U	rev ish enh(2p15p22, 17q22q25) dim(1p31p36) amp(2p23p24)
NBL-Meta-62	3	3	12	0	19	0	19	—	U	rev ish enh(12q22q24) dim(1p34p36, 8p22p23, 16) amp(2p24p25, 2p21)
NBL-Meta-63	3	3	48	0	41	0	41	—	U	rev ish enh(1p34q44, 2q23q37, 4, 12q21, 12q24, 17q22q25) dim(1p35p36, 15, 19, 20q, 22) amp(2p23p25)
NBL-Meta-64	3	3	23	1	1	1	1	—	U	rev ish enh(1p31q44, 2p11p21, 2q, 4, 13q32q34, 17q22q25, 18q) dim(1p32p36, 15q21q26, 20, 22) amp(2p23p25)
NBL-Meta-65	3	3	59	0	7	0	7	—	U	rev ish enh(1, 2q, 7, 17q22q25, 21) dim(8p22p23, 14q12q32, 15q15q26, 17p12p13, 19) amp(2p23p25)
NBL-Meta-66	2	3	59	1	59	0	82	—	U	rev ish enh(1q21q32, 7, 12q22q24, 17q22q25, 18q) dim(11q14q25)
NBL-Meta-67	3	3	52	1	18	1	18	—	—	rev ish enh(1q, 2p21q37, 3, 7, 9q32q34, 17q22q25, 18) dim(10q23q26) amp(2p23p25)
NBL-Meta-68	3	3	52	1	9	1	18	—	—	rev ish enh(1q, 2p21q37, 3, 7, 9q32q34, 17q22q25, 18) dim(10q23q26) amp(2p23p25)
NBL-Meta-69	1	3	19	0	88	0	88	—	U	rev ish enh(1, 2, 7, 13, 17, 18) dim(3, 4, 9)
NBL-Meta-70	3	4	19	1	8	1	8	—	—	rev ish enh(17q21q25) dim(1p34p36) amp(2p23p25)
NBL-Meta-71	4	4	38	1	8	1	8	—	—	rev ish enh(11p, 17q22q25) dim(3p21p26, 11q21q25) amp(16q21q24)
NBL-Meta-73	3	4	122	0	13	0	13	—	U	rev ish enh(1p12p22, 1q, 2p23p25, 12, 17q22q25) dim(1p31p36)
NBL-Meta-74	2	4	3	0	19	0	19	—	—	rev ish enh(17) dim(3, 4, 11, 14, 15)
NBL-Meta-75	2	4	66	0	18	0	18	—	U	rev ish enh(6q, 17q22q25, 18) dim(3, 5q, 11q22q25, 12q23q24)
NBL-Meta-76	3	4	51	0	4	0	4	—	—	rev ish enh(4q, 7q, 13q14q34, 17q22q25) dim(1p31p36, 10, 11q21q25, 16q22q24, 17p, 19) amp(2p23p25, 3q25q27)
NBL-Meta-77	3	4	31	1	22	1	22	—	U	rev ish enh(17q22q25) dim(1p31p36, 9p21p24) amp(2p23p25)
NBL-Meta-78	3	4	42	1	1	1	1	—	U	rev ish enh(4, 11q14q25, 17q21q25) dim(1p32p36, 17p, 19) amp(2p22p25)
NBL-Meta-79	3	4	61	1	12	1	12	—	U	rev ish enh(3q26q29, 4q, 10p, 17q22q25) dim(1p31p36, 3p26q25, 7q32q36, 10q22q34, 17p) amp(2p23p24)
NBL-Meta-80	3	4	20	1	7	1	7	—	U	rev ish enh(1q, 17q22q25) amp(2p23p24)
NBL-Meta-81	3	4S	3	0	19	0	19	—	F	rev ish enh(1q23q44, 2p21p25, 17q22q25) dim(1p31p36, 11q22q25, 14q21q32)
NBL-Meta-82	3	4S	1	0	75	0	75	—	—	rev ish enh(9q33q34, 17q22q25) dim(1p32p36) amp(2p22p24)
NBL-Meta-83	3	4S	1	1	17	1	17	—	U	rev ish enh(3q24q29) dim(1p34p36) amp(2p23p25)
NBL-Meta-84	1	4S	10	0	74	0	74	—	—	rev ish enh(7, 13q21q34, 17) dim(3, 4, 14)
NBL-Meta-86	3	4S	4	1	1	1	1	—	U	rev ish enh(13, 17q22q25) dim(1p35p36, 9, 14, 16p) amp(2p23p25)
NBL-Meta-87	1	4S	6	0	78	0	78	—	U	rev ish enh(1q, 5, 6, 7, 8, 9, 12, 13, 14q12q21, 17, 18) dim(1p, 14q22q32, 16)
NBL-Meta-88	3	4S	2	0	67	0	67	—	U	rev ish enh(2, 7, 13, 17, 18, 20, 21) dim(11, 19)
NBL-Meta-90	1	4S	2	0	49	0	49	—	U	rev ish enh(6, 7, 13, 15, 17, 18) dim(4, 5, 14, 21)
NBL-Meta-91	1	4S	1	0	46	0	46	—	U	rev ish enh(2, 6, 7, 12, 13, 17, 18) dim(3)

(continued on following page)

Mining of Neuroblastoma CGH Data

Supplemental Table: Clinical, Genetic, and Histopathologic Parameters and CGH Aberrations for 231 Primary Untreated Neuroblastomas (continued)

Identifier	Cluster ^a	Stage	Age ^b	Event ^c	EFS ^d	Survival ^e	OS ^f	Ploidy ^g	INPC ^h	CGH Aberrations
NBL-Meta-92	1	4S	3	0	36	0	36	—	U	rev ish enh(1, 2, 5, 6, 7, 12, 17, 19) dim(3, 4, 8, 9, 10, 11, 14, 18q, 21)
NBL-Meta-93	1	4S	8	0	70	0	70	—	U	rev ish enh(16p, 17, 19) dim(4q)
NBL-Meta-94	3	4S	4	1	9	1	9	—	F	rev ish enh(8p, 9q33q34, 12q22q24, 16, 17q22q25, 19, 21) dim(1p31p36, 4, 5, 6q12q21, 13q21q34, 18) amp(2p23p25)
NBL-Meta-95	1	4S	1	0	20	0	20	—	—	rev ish enh(2p, 6p21p23, 7, 9q32q34, 12, 17, 19, 20, 22) dim(3q, 4, 5q13q14, 8, 9p22p24, 14)
NBL-Meta-97	1	4S	3	0	2	0	2	—	—	rev ish enh(1, 2, 6, 7, 10, 12, 13, 17, 18, 20, 22) dim(3, 4, 5, 11, 14)
NBL-Meta-98	1	4S	4	0	7	0	7	—	U	rev ish enh(7, 12q23q24, 16, 17, 20q, 22) dim(3, 4, 8, 10, 11, 14q21q32, 15q15q26)
NBL-Meta-99	1	4S	8	0	5	0	5	—	U	rev ish enh(2, 6, 7, 9q22q34, 17, 18p, 22) dim(3, 4, 5, 8q, 11, 14q13q32)
NBL-Meta-100	1	4S	7	0	14	0	14	—	—	rev ish enh(6p, 7, 12q22q24, 17, 18p, 20, 22) dim(3, 4, 8q, 9, 10, 11, 13q14q22, 14q13q24)
NBL-Meta-101	1	1	11	0	30	0	30	—	—	rev ish enh(7, 15, 17, 22) dim(9q31q34, 14, X)
NBL-Meta-102	3	1	10	0	41	0	41	—	—	rev ish enh(2, 12q, 17q) dim(9p, 10)
NBL-Meta-104	1	2	9	0	54	0	54	—	—	rev ish enh(7, 17, 19) dim(4, 11, X)
NBL-Meta-105	1	2	8	0	83	0	83	tri	—	rev ish enh(1, 6p, 6q21q27, 7, 11q13, 11p15, 12, 17) dim(4, 21, X)
NBL-Meta-106	1	2	10	0	15	0	15	—	—	rev ish enh(2, 17, 19, 21q22, 22q13) dim(3, 4, 9p, 9q12q32, 11, 14, X)
NBL-Meta-107	3	4S	8	0	61	0	61	di	—	rev ish enh(16, 17, 22q13) dim(1p36, 6q12q21, X) amp(2p23p24)
NBL-Meta-108	1	4S	7	0	40	0	40	tri	—	rev ish enh(17)
NBL-Meta-109	1	3	24	1	3	1	3	tri	—	rev ish enh(17, 19, 22) dim(X)
NBL-Meta-110	3	3	60	0	36	0	36	—	—	rev ish enh(17q21q25) dim(1p, 3p24p26, 4p14p16) amp(2p24)
NBL-Meta-111	1	3	11	0	45	0	45	—	—	rev ish enh(6, 17) dim(4, 10q25q26)
NBL-Meta-112	1	3	9	0	64	0	64	tri	—	rev ish enh(7, 8p, 17) dim(10p, X)
NBL-Meta-113	3	4	12	0	42	0	42	tetra	—	rev ish enh(2p23, 6, 12p, 12q12q24, 17q22q25) dim(1p36, 4p, 9q32q34, 14, 18q22q23, 20)
NBL-Meta-114	3	4	90	1	28	1	28	—	—	rev ish enh(7, 17q22q25) dim(1p, 10q21q26, 18q22q23, X) amp(2p24)
NBL-Meta-115	1	4	24	1	11	1	11	—	—	rev ish enh(2p21p24, 5q32q35, 6p21, 12q24, 17, 19, 22) dim(1p13p32, 2q22q37, 3p21p26, 5p, 5q11q31, 9p21p24, 11q14q25, 13q21q34)
NBL-Meta-116	2	4	156	1	2	1	2	—	—	rev ish enh(12q24, 17q22q25) dim(3p24p26, 4p, 11q21q25)
NBL-Meta-117	3	4	30	1	11	1	11	di	—	rev ish enh(11q13, 17q21q25, 19) dim(1p36) amp(2p24)
NBL-Meta-118	4	4	240	0	21	0	21	di	—	rev ish dim(5q34q35)
NBL-Meta-119	1	4	10	0	24	0	24	—	—	rev ish enh(2p, 2q11q31, 7, 17, 21q21q22) dim(3, 4, 8, 9p, 11, 13q14q34)
NBL-Meta-120	3	4	24	1	9	1	9	di	—	rev ish enh(17q21q25) dim(1p21p36, X) amp(2p24)
NBL-Meta-121	4	4	216	1	18	1	24	—	—	rev ish enh(1p31q44, 4q12q31, 6p22p25, 12, 17q22q25) dim(1p32p36, 3, 6q21q27, 14q21q32, X)
NBL-Meta-122	1	4	41	1	10	1	13	—	—	rev ish enh(1p32p36, 1q, 7, 17q12q25, 19) dim(9p, 14, 18q, 21)
NBL-Meta-124	2	1	8	0	39	0	39	—	—	rev ish enh(7, 8, 17q) dim(2q22q37, 3, 4, 10, 11, 14)
NBL-Meta-125	4	1	14	0	51	0	51	—	—	rev ish enh(3, 7, 8, 12, 18) dim(10, 14, X)
NBL-Meta-126	1	1	6	0	36	0	36	—	—	rev ish enh(6, 7, 8, 12, 13, 15, 17q, 18q) dim(X)
NBL-Meta-127	1	1	2	0	46	0	46	tri	—	rev ish enh(6, 7, 12, 17)
NBL-Meta-128	1	1	4	0	36	0	36	tri	—	rev ish enh(1, 2, 7, 12, 17) dim(3, 4, 11, 14, X)
NBL-Meta-129	1	1	1	1	12	0	30	tri	—	rev ish enh(7, 12, 13, 17, 18, 22) dim(3, 4, 9, 10, 14)
NBL-Meta-130	1	1	5	0	24	0	24	—	—	rev ish enh(6, 7, 12, 13, 17, 18, 20, 22) dim(3, 14)
NBL-Meta-131	1	1	13	0	18	0	18	tetra	—	rev ish enh(5, 7, 17) dim(10, X)
NBL-Meta-132	1	1	1	0	13	0	13	tri	—	rev ish enh(6, 7, 12, 17, 18, 19) dim(4, 8, 14)
NBL-Meta-133	1	1	12	1	4	0	20	tri	—	rev ish enh(2p23p25, 6, 16, 17, 22) dim(3, 4, 9, 11, 14, X)
NBL-Meta-134	4	1	43.9	0	127.8	0	127.8	di	U	rev ish enh(7, 12, 20)
NBL-Meta-135	1	1	20.9	0	110.4	0	110.4	tri	F	rev ish enh(6, 7, 10, 12, 15, 17) dim(3, 4, 14, X)
NBL-Meta-136	1	1	4.5	0	116.8	0	116.8	tetra	F	rev ish enh(7, 8, 17, 22) dim(3, 4, 11, X)
NBL-Meta-137	1	1	1.4	1	51.5	0	85.8	tri	F	rev ish enh(2, 5, 7, 8, 13, 17) dim(3, 4, X)
NBL-Meta-139	1	1	48.3	0	74.1	0	74.1	—	F	rev ish enh(17)
NBL-Meta-140	2	1	93.5	1	15.1	1	73.6	—	—	rev ish enh(1q, 7, 11p15, 17q12q25, 18) dim(3p, 11q14q25)
NBL-Meta-141	1	2	4.3	0	62.2	0	62.2	tri	U	rev ish enh(2, 6, 7, 8, 17, 19, 20, 22) dim(3, 4, 9, 11)

(continued on following page)

Supplemental Table: Clinical, Genetic, and Histopathologic Parameters and CGH Aberrations for 231 Primary Untreated Neuroblastomas (continued)

Identifier	Cluster ^a	Stage	Age ^b	Event ^c	EFS ^d	Survival ^e	OS ^f	Ploidy ^g	INPC ^h	CGH Aberrations
NBL-Meta-142	1	2	13.6	1	17.2	0	64.7	di	U	rev ish enh(1, 2, 6, 7, 8, 17) dim(3, 4, 11, 14, 15)
NBL-Meta-143	1	2	8.1	0	47	0	47	tri	F	rev ish enh(6, 7, 15, 17, 22) dim(3, 4)
NBL-Meta-144	1	2	17	1	22	0	41	tri	—	rev ish enh(6, 7, 8, 17, 22) dim(3, 4, 11, 14, X)
NBL-Meta-145	1	2	13.7	1	1.1	0	57.6	tri	F	rev ish enh(1p32p36, 7, 12, 17, 19, 22) dim(3, 4, 5, 9, 11, 14, X)
NBL-Meta-146	1	2	19	0	116	0	116	—	—	rev ish enh(5, 6, 7, 13, 15, 17, 18) dim(19, X)
NBL-Meta-147	1	2	2	0	51	0	51	—	—	rev ish enh(6, 7, 9, 12, 17, 18) dim(4, 14, 21, X)
NBL-Meta-148	1	2	4	1	4	0	42	—	—	rev ish enh(6, 7, 17, 20) dim(1p36, 3, 4, 9, 10, 14)
NBL-Meta-149	2	2	23	1	5	0	27	—	—	rev ish enh(7, 17q) dim(1p36, 2q, 2p11p12, 3, 4, 8, 10, 12)
NBL-Meta-150	2	2	5	1	4	0	27	—	—	rev ish enh(17q21q25) dim(11q14q25)
NBL-Meta-151	1	2	17	0	28	0	28	—	—	rev ish enh(7, 13, 17q21q25) dim(11q14q25, 14q22q32)
NBL-Meta-153	1	2	9	0	24	0	24	tri	—	rev ish enh(7, 13, 17) dim(3, 4, 14)
NBL-Meta-154	1	2	12	0	54	0	54	tri	—	rev ish enh(6, 7, 17, 22) dim(3, 4, 9, 11, 14)
NBL-Meta-155	3	2	21	0	58	0	58	—	—	rev ish enh(1p35q44, 2p22q37, 7, 17q) dim(X) amp(2p23p25)
NBL-Meta-156	3	2	4	1	6	1	12	di	—	rev ish enh(17q22q25) dim(1p32p36) amp(2p23p25)
NBL-Meta-157	1	2	1	0	20	0	20	—	—	rev ish enh(2, 5, 7, 13, 17, 18) dim(3, 11, X, Y)
NBL-Meta-158	1	2	3	0	32	0	32	—	—	rev ish enh(1, 2, 5, 12, 13, 17) dim(3, 14, X)
NBL-Meta-159	1	2	24	0	18	0	18	di	—	rev ish enh(7, 15, 17, 18, 22) dim(11, 14, X)
NBL-Meta-160	1	2	39	0	13	0	13	di	—	rev ish enh(1, 7, 13, 15, 17, 18, 22) dim(3, 9, 11, 14, 21)
NBL-Meta-161	3	3	47	1	3	1	4	—	—	rev ish enh(7q32q36, 13) dim(1p33p36, 7p22q31, 8q24, 9p22p24, 11p, 12p13q23, 14, 15, 16, 17p12p13, 18, 20, 21, X) amp(2p23p25)
NBL-Meta-162	1	3	16	0	72	0	72	—	—	rev ish enh(7, 8, 13, 17, 18) dim(3, 11, X)
NBL-Meta-163	1	3	16	1	14	1	21	—	—	rev ish enh(5, 6, 7, 12, 13, 17, 18) dim(4, 8, 14, Y)
NBL-Meta-165	3	3	22	1	17	1	20	—	—	rev ish enh(6p, 7q, 8, 17q21q25, 18) dim(1p22p36, Y) amp(2p23p25)
NBL-Meta-167	1	3	3	0	12	0	12	—	—	rev ish enh(1, 2, 6, 7, 13, 17, 20) dim(11, 14, Xq)
NBL-Meta-168	1	3	21	0	26	0	26	—	—	rev ish enh(1, 7, 13, 15, 17, 18) dim(3, 9, 11, 14)
NBL-Meta-169	3	3	2	1	2.4	1	2.4	—	—	rev ish enh(17q21q25) dim(1p34p36) amp(2p24p25)
NBL-Meta-170	1	3	139.9	1	24	1	131.3	tri	—	rev ish enh(1, 2q, 7, 10, 11q12q22, 12q24, 15, 17q, 18, Xp11p21) dim(2p, 3, 4, 9, 11q23q25, 14, 21, Xq)
NBL-Meta-171	1	4	16	0	45	0	45	—	—	rev ish enh(1, 6, 7, 8, 13, 17, 22) dim(3, 11)
NBL-Meta-172	2	4	20	1	7	1	9	—	—	rev ish enh(1q25q44, 17q21q25) dim(1p31p36) amp(4q33q35)
NBL-Meta-173	2	4	67	1	17	1	20	—	—	rev ish enh(4q28q35, 5q31q35, 17q21q25, 18) dim(2, 3p14p26, 4p, 10, 11q13q25, 14q21q32) amp(6p12p21)
NBL-Meta-174	3	4	5	1	18	1	41	—	—	rev ish enh(6p21q27, 17q) dim(1p33p36, 10) amp(2p23p25)
NBL-Meta-175	2	4	39	1	6	1	6	di	—	rev ish enh(7, 17q21q25, 18) dim(11q14q25)
NBL-Meta-177	2	4	60	1	32	1	40	di	—	rev ish enh(1q, 7, 8, 17q, 18) dim(3, 9, 10q23q26, 11q21q25, Y)
NBL-Meta-178	1	4	9	0	48	0	48	tri	—	rev ish enh(2, 6, 7, 12, 13, 17q22q25)
NBL-Meta-179	2	4	29	1	12	1	12	—	—	rev ish enh(1p34q44, 6p, 7, 17q22q25, 18, 22) dim(1p35p36, 3, 4, 6q14q27, 8, 9, 10, 14, 15, 16, X)
NBL-Meta-180	3	4	61	0	9	0	9	tetra	—	rev ish enh(1p35q44, 2p22q37, 7, 17q, X) dim(1p36, 3, 5, 10, 15) amp(2p23p25)
NBL-Meta-181	4	4	20	1	10	1	15	di	—	rev ish enh(1q, 8q22q23) dim(1p, 8q24, 9p21p24) amp(4q33q35)
NBL-Meta-182	1	4S	6	1	3	0	36	tetra	—	rev ish enh(1p32q44, 2, 5, 6, 7, 12, 13, 17q21q25, 18) dim(1p33p36, 3p13p26, 15)
NBL-Meta-183	4	4	31.8	1	14.8	0	92.8	di	U	rev ish enh(8) amp(5q33q35)
NBL-Meta-184	3	4	9.1	1	11.4	1	15.6	—	U	rev ish enh(17q12q25) dim(1p) amp(2p24p25)
NBL-Meta-185	3	4	18.4	1	6	1	9	—	—	rev ish enh(1q, 2, 16, 17q22q25, 18q)
NBL-Meta-186	3	4	38	1	10.2	1	10.2	—	—	rev ish enh(1p31q44, 3, 5, 17q, 18q22q23) dim(1p32p36, 18p11q21) amp(2p23p25)
NBL-Meta-187	2	4	46.3	0	124.7	0	124.7	—	—	rev ish enh(17q, 22) dim(4q31q35, 11q14q25)
NBL-Meta-188	3	4	32.6	1	9.7	1	17.7	di	—	rev ish enh(1q, 17q) dim(1p, 8, 11) amp(2p24p25)
NBL-Meta-189	3	4	56.6	1	27.9	1	34.5	tetra	—	rev ish enh(1q, 2p22q37, 7, 8, 17q) dim(1p12p34, 3, 9, 11, 13q21q34, 14, 15, 18, X) amp(2p23p25)
NBL-Meta-190	3	4	36.4	1	15.7	1	15.7	—	—	rev ish enh(1q, 18q) dim(1p36) amp(2p23p25)
NBL-Meta-191	3	4	45	1	14	1	19	di	—	rev ish enh(6p, 11q, 17q24q25) dim(1p36, 6q22q27) amp(2p23p25)
NBL-Meta-192	1	4	60	0	36	0	36	di	—	rev ish enh(7, 11q13, 17q12q25, 19) dim(3p21p26, 4p15p16, 11q14q25, 14q24q32, 21)
NBL-Meta-193	4	4S	4	1	6	1	18	—	—	rev ish enh(1p31q44, 2p16p25, 6, 7, 12) dim(1p33p36, 10q)

(continued on following page)

Mining of Neuroblastoma CGH Data

Supplemental Table: Clinical, Genetic, and Histopathologic Parameters and CGH Aberrations for 231 Primary Untreated Neuroblastomas (continued)

Identifier	Cluster ^a	Stage	Age ^b	Event ^c	EFS ^d	Survival ^e	OS ^f	Ploidy ^g	INPC ^h	CGH Aberrations
NBL-Meta-194	1	4S	2	1	5	0	47	—	—	rev ish enh(2p21p25, 3p21q29, 6, 7, 12, 17q21q25, 18q) dim(1p32p36, 19, 22)
NBL-Meta-195	1	4S	6	0	52	0	52	—	—	rev ish enh(7, 17) dim(4, 5q11q23, 11, Xp)
NBL-Meta-197	1	4S	4	0	19	0	19	—	—	rev ish enh(10, 15, 17, 20q, 22) dim(11, 14, X)
NBL-Meta-200	3	4S	2.9	1	7.7	1	15.4	di	—	rev ish enh(2p21p25) dim(1p35p36)
NBL-Meta-201	1	4S	0.3	0	43.6	0	43.6	di	—	rev ish enh(2p16p25, 12q15q24, 17) dim(4p15p16)
NBL-Meta-202	1	4S	6.8	0	141.4	0	141.4	—	—	rev ish enh(1q, 2, 6, 7, 10, 13, 17) dim(3, 4, 8, 14)
NBL-Meta-203	1	4S	6.8	0	118.4	0	118.4	di	U	rev ish enh(2, 7, 12, 17) dim(3, 4, 5, 9, 10, 14)
NBL-4-01	2	4	61	1	5	1	10	—	—	rev ish enh(17q21q25) dim(11q21q25)
NBL-4-02	2	4	34	1	3	1	5	—	—	rev ish enh(1q11q44, 7, 13) dim(1p11p36, 4p11p16, 3, 8, 9, 10, 11, 16)
NBL-4-03	3	4	36	1	6	1	7	—	—	rev ish dim(1p34p36, 4p15p16)
NBL-4-04	2	4	54	1	7	1	20	—	—	rev ish enh(2p14p25, 17q11q25, 13) dim(9p12p24, 11q14q25)
NBL-4-05	2	4	29	1	14	1	16	—	—	rev ish enh(17q22q25) dim(11q14q25)
NBL-4-06	2	4	12	1	8	1	8	—	—	rev ish enh(17q11q25) dim(11q14q25)
NBL-4-07	4	4	88	1	2	1	4	—	—	rev ish dim(3p11p26, 11q21q25, 17p11p13)
NBL-4-08	3	4	27	1	10	1	10	—	—	rev ish enh(17q11q25, 2, 7) dim(8, 9, 11)
NBL-4-09	2	4	38	1	11	1	11	—	—	rev ish enh(6q23q37, 11p11p15, 17q11q25) dim(3p11p26, 4p14p16, 8p11p23, 11q14q25)
NBL-4-10	2	4	64	0	6	0	6	—	—	rev ish enh(2p22p25, 13q21q34, 17q22q25) dim(3p21p26, 4p15p16, 11q14q25)
NBL-4-11	2	4	57	0	8	0	8	—	—	rev ish enh(7q21q36, 17q21q25, 18) dim(11q14q25)
NBL-4-12	2	4	41	1	19	1	20	—	—	rev ish enh(17q11q25, 13, 18) dim(3p11p26, 11q14q25, 14q24q32, 17p11p13, 10)
NBL-4-13	4	4	38	0	9	0	9	—	—	rev ish enh(6p22p25, 7p11p14, 7q11q36, 17q11q25, 13) dim(4q31q35)
NBL-4-14	2	4	9	0	51	0	51	—	—	rev ish dim(11q14q25)
NBL-4-41	3	4	28	0	14	0	14	—	—	rev ish enh(2p22p25, 7q21q36, 17q21q25) dim(1p32p36, 4p12p16, 10p11p15, 14q22q34)
NBL-4-42	4	4	19	0	16	0	16	—	—	rev ish enh(4q11q35, 5q11q23, 13q14q34) dim(4p14p16, 17p11p13, 16, 19, 20, 22)
NBL-4-43	2	4	65	1	10	0	22	—	—	rev ish enh(12q21q24, 17q11q25) dim(6q24q27, 17p11p13)
NBL-4-44	2	4	44	1	22	0	22	—	—	rev ish enh(1q11q44, 13q33q34, 17q11q25) dim(9p11p24, 11q14q25, 16q11q24)
NBL-4-45	2	4	36	0	8	0	8	—	—	rev ish enh(2p15p25, 7q21q26, 17q11q25) dim(11q14q25)
NBL-4-46	2	4	156	0	67	0	67	—	—	rev ish enh(2p21p25, 10p11p15, 17q11q25, Xp11p22, 17, 18) dim(3q11q29, 6p11p25, 11q14q25) amp(14q12q13)
NBL-4-47	4	4	84	0	22	0	22	—	—	rev ish enh(2p16p25, 7q22q26) dim(11q21q25, 14q22q32, 3)
NBL-4-48	2	4	96	0	41	0	41	—	—	rev ish enh(17q21q25) dim(14q22q32)
NBL-4-49	2	4	84	0	6	0	6	—	—	rev ish enh(17q21q25, Xp11p22, 18) dim(3p14p26)
NBL-4-50	2	4	47	1	1	1	4	—	—	rev ish enh(17q21q25, 13) dim(11q14q25)
NBL-4-52	3	4	67	0	10	0	10	—	—	rev ish enh(7q11q26, 16q22q24, 17q11q25, 12) dim(1p32p36, 4p11p16, 17p11p13, 11) amp(2p24p25)
NBL-01	3	2	6.5	0	156	0	156	—	—	rev ish enh(2, 7, 17, 18)
NBL-03	1	2	9	0	30	0	30	—	F	rev ish enh(1, 2, 6, 7, 10, 12, 17, 18) dim(19)
NBL-04	1	2	28.9	0	108	0	108	—	—	rev ish enh(6, 7, 13, 17, 18) dim(19)
NBL-05	3	2	0.5	0	120	0	120	—	U	rev ish enh(1, 2, 5, 7, 9, 10, 12, 15, 17, 20, 22)
NBL-06	4	2	54.1	1	8	1	9	—	U	rev ish enh(2, 3q22qter, 6p, 7q21qter, 12q13q15, 17q) dim(2q33q35, 10) amp(2p24pter)
NBL-07	3	3	1.4	0	48	0	48	—	—	rev ish enh(1, 2, 7, 8)
NBL-09	2	4	13.8	NA	NA	1	10	—	U	rev ish enh(17q, 18q) dim(1p32pter) amp(2p24pter, 11q12q14)
NBL-10	3	4	30.7	0	43	0	43	—	U	rev ish enh(1q, 2, 3p14qter, 4q, 6, 7, 8, 9q, 10q, 11p, 12, 13, 14, 16q, 17q, 18q, 20, 21, 22, Xp) dim(3p21pter, 4p, 11q22qter) amp(2p24pter, 12q23)
NBL-11	3	4	59.4	1	11	1	23	—	U	rev ish enh(1q, 2p24pter, 4q31q31, 5p15, 5q31, 7q, 12, 16, 17q, 18q, 20q, 22, Xp22)
NBL-12	3	4S	1.8	0	31	0	31	—	—	rev ish enh(1, 2, 9, 13, 15, 17)
NBL-13	4	4	32.4	1	27	1	40	—	—	rev ish enh(6p, 9q11, 15, Xp22)
NBL-14	3	4	24.6	1	13	1	14	—	U	rev ish enh(2p13pter, 17q) dim(1p32pter) amp(2p24pter)
NBL-15	2	4	23.8	1	19	1	22	—	U	rev ish enh(17q) dim(17p) amp(2p24pter)
NBL-16	3	4	11.3	1	13	1	16	—	U	rev ish enh(1p31qter, 2, 3, 4, 5, 6, 7, 8, 9, 10, 11, 12, 13, 14, 15, 16, 17q, 18q, 19, 20, 21, 22) amp(2p24pter)

(continued on following page)

Supplemental Table: Clinical, Genetic, and Histopathologic Parameters and CGH Aberrations for 231 Primary Untreated Neuroblastomas (continued)

Identifier	Cluster ^a	Stage	Age ^b	Event ^c	EFS ^d	Survival ^e	OS ^f	Ploidy ^g	INPC ^h	CGH Aberrations
NBL-17	4	4	39.6	0	36	0	36	—	U	rev ish enh(2p21pter) dim(1p31pter, 3p21pter, 11q22qter, 19)
NBL-18	1	2	0.4	0	19	0	19	—	U	rev ish enh(5, 6, 12, 17, 18)
NBL-19	4	4S	1.2	1	6	0	30	—	U	rev ish enh(1p32qter, 7, 12)
NBL-20	3	3	23	0	96	0	96	—	—	rev ish enh(1q, 2, 5, 12q21q23, 13, 14, 17q, 18, 20, 21, 22) dim(1p32pter, 10q24qter) amp(2p24pter)
NBL-21	3	4	18.6	NA	NA	1	19	—	—	rev ish enh(1, 5, 9, 14, 15, 17, 20, 22)
NBL-22	2	4	36	NA	NA	1	27	—	—	rev ish enh(7, 8p22pter, 17q, 18) dim(3p24pter, 11q22)
NBL-23	3	4	88.9	NA	NA	1	29	—	U	rev ish enh(1, 2, 9q, 10, 12q, 13, 14, 16, 17q, 18q, 20, 21, 22, Xp)
NBL-24	2	3	47.3	1	16	1	23	—	—	rev ish enh(17q, 18p11.3) dim(4p13, 9q34, 11q22qter) amp(11q13q14)

^aAccording to Figure 2A, 4 = not belonging to cluster 1, 2 or 3; ^bage at diagnosis (months); ^c1 = tumor progression, relapse or death, 0 = no event, — = not available; ^devent-free survival (months) (see Materials and Methods), — = not available; ^e1 = death, 0 = alive; ^foverall survival (months); ^gdi = near-diploid, tetra = near-tetraploid, tri = near-triploid, — = not available; ^hF = favorable risk status, U = unfavorable, — = not available.

REFERENCES

- Seeger RC, Brodeur GM, Sather H, et al: Association of multiple copies of the N-myc oncogene with rapid progression of neuroblastomas. *N Engl J Med* 313:1111-1116, 1985
- Fong CT, Dracopoli NC, White PS, et al: Loss of heterozygosity for the short arm of chromosome 1 in human neuroblastomas: Correlation with N-myc amplification. *Proc Natl Acad Sci U S A* 86:3753-3757, 1989
- Look AT, Hayes FA, Shuster JJ, et al: Clinical relevance of tumor cell ploidy and N-myc gene amplification in childhood neuroblastoma: A Pediatric Oncology Group study. *J Clin Oncol* 9:581-591, 1991
- Bown N: Neuroblastoma tumour genetics: Clinical and biological aspects. *J Clin Pathol* 54:897-910, 2001
- Maris JM, Matthay KK: Molecular biology of neuroblastoma. *J Clin Oncol* 17:2264-2279, 1999
- Westermann F, Schwab M: Genetic parameters of neuroblastomas. *Cancer Lett* 184:127-147, 2002
- Ejeskar K, Aburatani H, Abrahamsson J, et al: Loss of heterozygosity of 3p markers in neuroblastoma tumours implicate a tumour-suppressor locus distal to the FHIT gene. *Br J Cancer* 77:1787-1791, 1998
- Guo C, White PS, Weiss MJ, et al: Allelic deletion at 11q23 is common in MYCN single copy neuroblastomas. *Oncogene* 18:4948-4957, 1999
- Takita J, Hayashi Y, Kohno T, et al: Allelo-type of neuroblastoma. *Oncogene* 11:1829-1834, 1995
- Luttikhuis ME, Powell JE, Rees SA, et al: Neuroblastomas with chromosome 11q loss and single copy MYCN comprise a biologically distinct group of tumours with adverse prognosis. *Br J Cancer* 85:531-537, 2001
- Bown N, Cotterill S, Lastowska M, et al: Gain of chromosome arm 17q and adverse outcome in patients with neuroblastoma. *N Engl J Med* 340:1954-1961, 1999
- Speleman F, Bown N: 17q gain in neuroblastoma, in Brodeur GM, Sawada T, Tsuchida Y, et al (eds): Neuroblastoma. Amsterdam, the Netherlands, Elsevier, 2000, pp 113-124
- Kallioniemi A, Kallioniemi OP, Sudar D, et al: Comparative genomic hybridization for molecular cytogenetic analysis of solid tumors. *Science* 258:818-821, 1992
- du Manoir S, Speicher MR, Joos S, et al: Detection of complete and partial chromosome gains and losses by comparative genomic in situ hybridization. *Hum Genet* 90:590-610, 1993
- Vandesompele J, Van Roy N, Van Gele M, et al: Genetic heterogeneity of neuroblastoma studied by comparative genomic hybridization. *Genes Chromosomes Cancer* 23:141-152, 1998
- Plantaz D, Mohapatra G, Matthay KK, et al: Gain of chromosome 17 is the most frequent abnormality detected in neuroblastoma by comparative genomic hybridization. *Am J Pathol* 150:81-89, 1997
- Lastowska M, Nacheva E, McGuckin A, et al: Comparative genomic hybridization study of primary neuroblastoma tumors: United Kingdom Children's Cancer Study Group. *Genes Chromosomes Cancer* 18:162-169, 1997
- Brinkschmidt C, Christiansen H, Terpe HJ, et al: Comparative genomic hybridization (CGH) analysis of neuroblastomas: An important methodological approach in paediatric tumour pathology. *J Pathol* 181:394-400, 1997
- Vandesompele J, Speleman F, Van Roy N, et al: Multicentre analysis of patterns of DNA gains and losses in 204 neuroblastoma tumors: How many genetic subgroups are there? *Med Pediatr Oncol* 36:5-10, 2001
- Plantaz D, Vandesompele J, Van Roy N, et al: Comparative genomic hybridization (CGH) analysis of stage 4 neuroblastoma reveals high frequency of 11q deletion in tumors lacking MYCN amplification. *Int J Cancer* 91:680-686, 2001
- Breen CJ, O'Meara A, McDermott M, et al: Coordinate deletion of chromosome 3p and 11q in neuroblastoma detected by comparative genomic hybridization. *Cancer Genet Cytogenet* 120:44-49, 2000
- Brinkschmidt C, Poremba C, Christiansen H, et al: Comparative genomic hybridization and telomerase activity analysis identify two biologically different groups of 4s neuroblastomas. *Br J Cancer* 77:2223-2229, 1998
- Baudis M, Cleary ML: Progenetix.net: An online repository for molecular cytogenetic aberration data. *Bioinformatics* 17:1228-1229, 2001
- Brodeur GM, Pritchard J, Berthold F, et al: Revisions of the international criteria for neuroblastoma diagnosis, staging, and response to treatment. *J Clin Oncol* 11:1466-1477, 1993
- Shimada H, Ambros IM, Dehner LP, et al: The International Neuroblastoma Pathology Classification (the Shimada system). *Cancer* 86:364-372, 1999
- Bentz M, Plesch A, Stilgenbauer S, et al: Minimal sizes of deletions detected by comparative genomic hybridization. *Genes Chromosomes Cancer* 21:172-175, 1998
- Dysvik B, Jonassen I: J-express: Exploring gene expression data using Java. *Bioinformatics* 17:369-370, 2001
- Holzman T, Kolker E: Statistical analysis of global gene expression data: Some practical considerations. *Curr Opin Biotechnol* 15:52-57, 2004
- Lastowska M, Cullinane C, Variend S, et al: Comprehensive genetic and histopathologic study reveals three types of neuroblastoma tumors. *J Clin Oncol* 19:3080-3090, 2001
- Abel F, Ejeskar K, Kogner P, et al: Gain of chromosome arm 17q is associated with unfavourable prognosis in neuroblastoma, but does not involve mutations in the somatostatin receptor 2(SSTR2) gene at 17q24. *Br J Cancer* 81:1402-1409, 1999
- Cunsolo CL, Bicocchi MP, Petti AR, et al: Numerical and structural aberrations in advanced neuroblastoma tumours by CGH analysis: Survival correlates with chromosome 17 status. *Br J Cancer* 83:1295-1300, 2000
- Spitz R, Hero B, Ernestus K, et al: Deletions in chromosome arms 3p and 11q are new prognostic markers in localized and 4s neuroblastoma. *Clin Cancer Res* 9:52-58, 2003
- Spitz R, Hero B, Ernestus K, et al: Gain of distal chromosome arm 17q is not associated with poor prognosis in neuroblastoma. *Clin Cancer Res* 9:4835-4840, 2003
- Mattfeldt T, Wolter H, Kemmerling R, et al: Cluster analysis of comparative genomic

hybridization (CGH) data using self-organizing maps: Application to prostate carcinomas. *Anal Cell Pathol* 23:29-37, 2001

35. Joos S, Menz CK, Wrobel G, et al: Classical Hodgkin lymphoma is characterized by recurrent copy number gains of the short arm of chromosome 2. *Blood* 99:1381-1387, 2002

36. Dyer S, Prebble E, Davison V, et al: Genomic imbalances in pediatric intracranial ependymomas define clinically relevant groups. *Am J Pathol* 161:2133-2141, 2002

37. Burton EC, Lamborn KR, Feuerstein BG, et al: Genetic aberrations defined by comparative genomic hybridization distinguish long-term from

typical survivors of glioblastoma. *Cancer Res* 62:6205-6210, 2002

38. Fritz B, Schubert F, Wrobel G, et al: Microarray-based copy number and expression profiling in dedifferentiated and pleomorphic liposarcoma. *Cancer Res* 62:2993-2998, 2002

39. Wang TL, Maierhofer C, Speicher MR, et al: Digital karyotyping. *Proc Natl Acad Sci U S A* 99:16156-16161, 2002

40. Pinkel D, Seagraves R, Sudar D, et al: High resolution analysis of DNA copy number variation using comparative genomic hybridization to microarrays. *Nat Genet* 20:207-211, 1998

41. Solinas-Toldo S, Lampel S, Stilgenbauer S, et al: Matrix-based comparative genomic hybridiza-

tion: Biochips to screen for genomic imbalances. *Genes Chromosomes Cancer* 20:399-407, 1997

42. Pollack JR, Perou CM, Alizadeh AA, et al: Genome-wide analysis of DNA copy-number changes using cDNA microarrays. *Nat Genet* 23:41-46, 1999

43. Lucito R, Healy J, Alexander J, et al: Representational oligonucleotide microarray analysis: A high-resolution method to detect genome copy number variation. *Genome Res* 13:2291-2305, 2003

44. Bignell GR, Huang J, Greshock J, et al: High-resolution analysis of DNA copy number using oligonucleotide microarrays. *Genome Res* 14:287-295, 2004.